Predictive channel reservation for handoff prioritization in wireless cellular networks

Zhenqiang Ye [a], Lap Kong Law [b,*], Srikanth V. Krishnamurthy [b], Zhong Xu [a], Suvidhean Dhirakaosal [b], Satish K. Tripathi [c], Mart Molle [b]

[a] *Department of Electrical Engineering, University of California, Riverside, CA 92521, United States*
[b] *Department of Computer Science and Engineering, University of California, Riverside, CA 92521, United States*
[c] *Department of Computer Science and Engineering, SUNY at Buffalo, Buffalo, NY 14260, United States*

Abstract

In wireless cellular networks, a roaming mobile station (MS) is expected to move from one cell to another. In order to ensure that ongoing calls are not dropped while the owner mobile stations roam among cells, handoff calls may be admitted with a higher priority than newly generated calls. Predictive channel reservation (or pre-reservation) schemes allow the reservation of a channel for an ongoing call in an adjacent cell before its owner MS moves into that cell, so that the call is sustained when the MS moves into the adjacent cell. Pre-reservations are made when the MS is within some distance of the new cell boundary. This distance determines the area in which the MS can make channel reservations. In this paper, we study the effect of the pre-reservation area size on handoff performance in wireless cellular networks. Our studies show that if the reserved channels are strictly mapped to the MSs that made the corresponding reservations, as we increase the pre-reservation area size, the system performance (in terms of the probability that the handoff calls are dropped) improves initially. However, beyond a certain point, the performance begins to degrade due to a large number of *false* reservations. The optimal pre-reservation area size is closely related to the traffic load of the network and the MSs' mobility pattern (moving speed). We provide an analytical formulation that furthers understanding with regard to the perceived behavior in one-dimensional networks (in which all cells are along a line).

With the objective of improving handoff performance and alleviating this sensitivity to the area size, we propose an adaptive channel pre-reservation scheme. Unlike prior pre-reservation methods, the key idea in our scheme is to send a channel pre-reservation request for a possible handoff call to a neighboring cell not only based on the position and orientation of the owner MS, but also as per its speed towards the target cell. The newly proposed scheme uses GPS measurements to determine when channel pre-reservation requests are to be made. Simulation results show that the adaptive channel pre-reservation scheme performs better in all typical scenarios than a previously proposed popular pre-reservation method that does not take mobility into account.

---

* Corresponding author. Tel.: +1 951 827 2434.
  E-mail addresses: zye@cs.ucr.edu (Z. Ye), lklaw@cs.ucr.edu (L.K. Law), krish@cs.ucr.edu (S.V. Krishnamurthy), zhong@cs.ucr.edu (Z. Xu), sdhirak@cs.ucr.edu (S. Dhirakaosal), tripathi@buffalo.edu (S.K. Tripathi), mart@cs.ucr.edu (M. Molle).

1. Introduction

When a mobile station (MS) with an ongoing call moves from a particular cell to its next target cell, if the target cell does not have sufficient bandwidth[1] (in terms of frequency bands if FDMA is deployed, time slots if TDMA is used, or code words if CDMA is used), the call will be dropped. Since dropping a handoff call is more annoying than blocking a new call from the user's perspective, several schemes [2–4,1,5] have been proposed to prioritize handoff calls.

Handoff prioritization schemes can be divided into two categories [5]: *static channel reservation* schemes and *dynamic channel reservation* schemes. The guarded channel (GC) scheme [2] is a popularly considered static channel reservation scheme. In the GC scheme, a certain number of channels are reserved exclusively for handoff requests. Even though the GC scheme can improve the success rate of handoff requests, it could decrease the system utilization due to an increased blocking probability of new calls. In dynamic channel reservation schemes, channels are dynamically reserved according to probabilistic predictions of MSs' movements. In the dynamic channel reservation schemes, usually a channel pre-reservation (PR) area is defined. The number of MSs with ongoing calls that are within the PR area and the corresponding probabilistic predictions of their motion are used to determine if channel pre-reservation requests are to be sent to adjacent cells.

In the dynamic channel reservation schemes, there are two approaches by which handoff calls access the dynamically reserved channels: the *non-sharing* approach and the *sharing* approach. In the *non-sharing* approach, each reserved channel is strictly mapped to the MS that made the corresponding channel pre-reservation request. A handoff call may be dropped when all channels are either being used or are being reserved (not actually being used). The *non-sharing* approach may gener-

ate large numbers of *false* reservations if the pre-reservation (PR) area size is large or if the MSs move with slow speeds. An extreme example is that a static MS that is within the PR area of a cell reserves a channel in the cell; however, the channel will never be used by the MS since the MS never moves into the cell. Thus, even though increasing the PR area size allows for possible handoff calls to make pre-reservations, it may cause a large numbers of *false* channel reservations. Large number of *false* reservations, in turn, increase the handoff call dropping probability and decrease the overall channel utilization. In the reserved channel *sharing* approach, the reserved channels are pooled for being allocated to any handoff call. The MSs with ongoing calls reserve channels when they move into the PR area. The reserved channels are grouped into a pool. A reserved channel is randomly assigned for use by a handoff call when its owner MS crosses the boundary from the previous cell to enter the new cell. Note that, with the *sharing* approach, the higher the number of channel pre-reservations, the lower the handoff call dropping probability. On the other hand, the more the reserved channels, the smaller the number of the channels that can be allocated to newly generated calls. There is a trade-off between decreasing the handoff call dropping probability and maintaining high channel utilization.

In the first part of this paper, we study the effects of the size of the PR area on the handoff prioritization performance if the *non-sharing* approach is used. We develop an analytical model for one-dimension cellular systems and perform simulations to verify the behavioral assessments from the one-dimensional model into the two-dimensional cellular systems. The studies show that there exists an optimal PR area size at which the handoff call dropping probability is minimized for a cellular system. The size of the optimal PR area is closely related to the MSs' mobility pattern (moving speed). Thus, a constant pre-reservation area may not be appropriate in a cellular system. In the second part of this paper, we propose an adaptive channel pre-reservation scheme. In our proposed scheme, the pre-reserved channels are shared by all handoff calls, i.e., the *sharing* approach is used. Instead of

---

[1] We will use *channel* to represent bandwidth in the rest of this paper.

defining a *constant* size for the PR area as in prior work [1], in our adaptive channel reservation scheme, we use a *threshold time* concept that dictates reservation requests. In the new scheme, the time at which a MS will move into a new cell is predicted and if this time is less than a pre-defined threshold, a channel pre-reservation request is sent to the new cell by the MS. The scheme integrates threshold time, reserved channel sharing and other features of the prior schemes [1] to minimize the effects of false reservations and improve the channel utilization of cellular systems. Simulation results show that our adaptive channel pre-reservation scheme performs better, in almost all typical scenarios, than the previously proposed predictive channel reservation (PCR) scheme in [1].

The reminder of this paper is organized as follows. In Section 2 we discuss related work on handoffs in cellular networks. The assumptions, policies and metrics of interest of the paper are discussed in Section 3. In Section 4, we provide an analytical model to analyze the impact of the size of the pre-reservation area on handoff prioritization performance in one-dimensional cellular systems. In Section 5, the effect of the pre-reservation area size on handoff prioritization performance is studied in two-dimensional cellular networks via simulations. Our proposed adaptive channel reservation scheme is discussed in Section 6 and its performance is evaluated. Finally, we conclude the paper in Section 7.

2. Related work

Many schemes have been proposed for the prioritization of handoff calls in wireless cellular systems [2,6–8,1,9]. As discussed in Section 1, there are two popular strategies employed to prioritize handoff calls: the *static channel reservation* strategy and the *dynamic channel reservation* strategy. The static channel reservation strategy decreases the handoff dropping probability by reserving a fixed number of channels exclusively for handoff calls. New calls are blocked if the number of idle channels is equal to or less than the number of guarded channels; handoff calls are served unless all of the channels are occupied. The dynamic channel reservation schemes adaptively adjust the number of reserved channels based on the traffic loads in adjacent cells. These two strategies can be combined to obtain better performance as compared with the individual strategies [1].

Since the behavior, in terms of mobility, of different MSs may differ and the offered traffic load in each cell varies from time to time, any static channel reservation scheme cannot work efficiently all the time. In order to solve this problem, several dynamic channel reservation schemes have been proposed [4,1,10,11,7–9,12]. The *shadow cluster* concept proposed in [4] allows the base station of each cell to calculate the probabilities of a given MS being active in other cells at future times; this thereby facilitates the prediction of future resource demands. In [11] a prediction algorithm is proposed to predict the next cell that a mobile user would move into using individual and aggregate user handoff profiles. The usefulness of MSs' mobility profiles are quantified in [10]. In [8], the number of guarded channels in each cell is adjusted according to the current estimate of handoff call arrival rate, which is in turn derived from the current number of ongoing calls in neighboring cells and the mobility patterns of the MSs. In [7], channels are dynamically reserved by using the *request probability* determined by the mobility patterns of the MSs and the current traffic load. All these schemes take into account the MSs' mobility patterns when they dynamically make channel reservations. But the mobility patterns that are considered are generic MS motion patterns, and they do not identify each individual MS's behavior in terms of mobility separately. In [1], the predictive channel reservation (PCR) scheme is proposed and it is based on mobile positioning. The *threshold distance* concept is used to define the size of a channel reservation area. The PCR scheme facilitates predictive channel reservations for each MS based on its current position and orientation. However, the threshold distance in the PCR scheme is chosen to be a constant for all MSs. Note that none of the previous efforts study the effect of the size of the PR area size on handoff prioritization performance.

Some work has been done in predicting the next target cells for given MSs, based on their motion in order to make accurate reservation decisions [13,14,12,9]. In this paper, we assume that the MSs' trajectory can be estimated accurately by using GPS or other positioning technologies. This assumption can alleviate the effect of false reservations to the maximum extent. Here a false reservation is defined as a reservation that is unused, i.e., a reservation that is made by a MS in a cell but after which the MS does not move to that cell, or the ongoing call for which the reservation was made

ends before the MS moved into that cell. The effect of false reservations that occur due to the first reason (i.e., the MS changes its direction of motion and therefore does not enter the cell in which the pre-reservation was made) can be alleviated by making accurate predictions about the MS's next target cell.

3. Assumptions, policies and metrics of interest

In dynamic channel reservation schemes, a pre-reservation area is usually defined [4,1]. In Fig. 1, there are two circles that are concentric with cell A. The radius of these circles are R_c and R_p, respectively. The area covered by the circle with radius R_c is the coverage area of cell A. The area between these two circles (the shared region) is defined to be the pre-reservation area. The MSs with ongoing calls that are located within the pre-reservation area need to decide whether or not to reserve channels in cell A.

3.1. Call admission control

We assume that every cell in the system is of the same size and has the same fixed number of channels. There are no guarded channels for handoff calls in any cell, i.e., both new and handoff calls have access to all the channels. Each MS is associated with at most one call at any given time. If a new call that is generated in a cell cannot find an idle channel in that cell, the call is discarded (blocked) immediately. There is no queue provided for new calls to wait. If a MS generates a new call in the PR area, and the new call is accepted by the current cell, or if a MS with an ongoing call moves

Fig. 1. The shaded region is the pre-reservation area of cell A.

into the PR area, a PR request is sent to the MS's next target cell. If there is an idle channel in this new cell, the request is accepted, and an idle channel is reserved for the call (if the *non-sharing* approach is used) or is inserted into the pool of reserved channels (if the *sharing* approach is used). If there is no idle channel in this new cell, the PR request is inserted into a queue (we assume that the queue size is infinite). The request will be dequeued if (a) the corresponding call is assigned a channel, (b) if the call is completed before its owner moves out of the PR area, or (c) if the call is dropped due to its owner MS moving into the cell prior to the request being honored. The channel reserved by a MS is released either if the MS's ongoing call ends before it moves into the new cell or if the MS changes its direction of motion and moves to a different new cell.

3.2. Reserved channel access approaches

As discussed in Section 1, there are two approaches for dictating how the handoff calls access the reserved channels: the *non-sharing* approach and the *sharing* approach. In the *non-sharing* approach, each reserved channel is strictly mapped (a one-to-one correspondence) to the MS that made the reservation. The reserved channel is precluded from being used by other handoff requests or new calls until it is released by the reserving MS. *Soft handoff* in CDMA cellular networks is one of the examples of where this approach is used [15]. In CDMA cellular networks, a MS can communicate with multiple base stations at the same time when it is located inside a so called boundary region of multiple cells. It adaptively chooses the BS with the best communication quality. In this case, it not only holds a channel in its primary cell, but also holds (or reserves) channels in other adjacent cells. The reserved channels cannot be shared by other MSs. In the reserved channel *sharing* approach, all reserved channels are pooled together. There is no strict mapping between the reserved channels and the reserving MSs. If a handoff is initiated, one of the reserved channels in the pool is randomly allocated to the handoff call and the number of reserved channels is decreased by one. This approach is also called reservation pooling [1]. Compared with the *non-sharing* approach, the reserved channel *sharing* approach provides a higher level of flexibility in the handling of handoff calls and always decreases the handoff call dropping probability. It does not mean that the *sharing* approach can
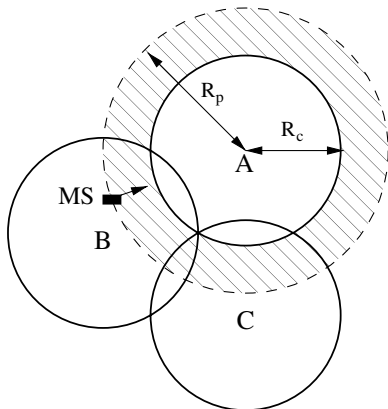
completely replace the *non-sharing approach* in cellular systems. For example, in order to achieve high quality communications, the MSs that are in handoff regions in CDMA cellular networks (the example that we previously discussed) may hold channels in multiple cells. The reserved channels, in this case, cannot be shared by other calls.

3.3. Performance metrics

In previous work, three metrics are typically considered to measure the performance of handoff in cellular systems:

- P_b denotes the new call blocking probability.
- P_d denotes the handoff call dropping probability.
- P_{nc} represents the probability that a call is not completed due to either being blocked or being dropped during handoff. We call it the *call incompletion probability*.

In this paper, we conform to the above performance metrics.

4. An analysis to understand the effect of the PR area size on handoff prioritization performance

In this section, we consider a one-dimensional cellular system and analyze the handoff performance. Our key objective is to examine the impact of the size of the pre-reservation area on performance in terms of the metrics listed in the previous section. Toward this we consider the simple non-sharing approach with Markovian models for various random variables of interest (to be discussed). We see that the analysis becomes quite involved even for this simpler system. As we show by simulations, the behavioral assessments remain the same even if more generic two-dimensional systems are considered.

The system under consideration for this analysis is depicted in Fig. 2. All the cells in the system are collocated along a line as shown. Each cell is divided into two areas: the non-PR area and the PR area. When a call is generated in the non-PR area of a given cell (consider cell k in Fig. 2), its owner MS does not need to send a PR request to the base station of the corresponding neighboring cell (cell $k-1$ or cell $k+1$). Once the owner of the call moves into the PR area (area $PR(k, k-1)$ or area $PR(k, k+1)$) from the non-PR area (area $NPR(k)$), it will send out a PR request to it's closest neighboring cell (cell $k-1$ or cell $k+1$). Note from the above notation that we use $NPR(i)$ to represent the non-PR area of cell i, and $PR(i, j)$ to represent the PR area of cell i, in which MSs send PR requests to cell j.

4.1. Assumptions and definitions

The assumptions that we make and variables that we define for the purpose of analyzing the performance of the system under consideration are listed below:
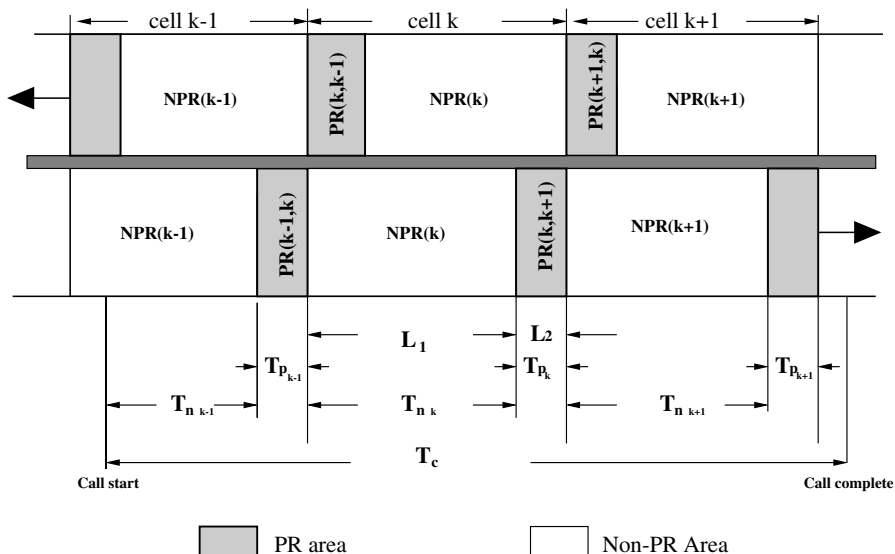

Fig. 2. Diagram of a one-dimensional cellular system.

- *Call holding time* T_c represents the duration of a call. It is assumed to be exponentially distributed with a probability density function (PDF) given by $f_{T_c}(t) = \mu e^{-\mu t}$.
- *A MS's non-PR area dwell time* T_n is the time that the MS stays in a non-PR area. We assume it to be exponentially distributed with a PDF given by $f_{T_n}(t) = \eta e^{-\eta t}$.

  Suppose a new call is generated when a MS is in a particular non-PR area; let T_{nn} denote the time interval from the moment that the call is generated to the moment that its owner leaves the non-PR area, i.e., T_{nn} is the residual dwell time of a MS in the non-PR area. It is shown in [16] that the PDF of this residual time is given by

$$f_{T_{nn}}(t) = \frac{1 - F_{T_n}(t)}{E[T_n]} = \eta e^{-\eta t}. \tag{1}$$

  Note that T_{nn} has the same distribution as T_n.
- *A MS's PR area dwell time* T_p is the time that the MS stays in a PR area. We assume that this random duration is exponentially distributed with a PDF given by $f_{T_p}(t) = \gamma e^{-\gamma t}$.

  Let us assume that a new call is generated when a MS is in a particular PR area; let T_{np} be the time interval from the moment that the new call is generated to the moment that its owner leaves this area. As in Eq. (1), the PDF of T_{np} is given by

$$f_{T_{np}}(t) = \frac{1 - F_{T_p}(t)}{E[T_p]} = \gamma e^{-\gamma t}. \tag{2}$$

  Note that T_{np} has the same distribution as T_p.
- The arrivals of new calls and PR calls in a cell are assumed to occur in accordance to Poisson processes with mean arrival rates of λ_n and λ_p, respectively.
- MSs are uniformly distributed in the wireless system under consideration. All MSs know their geographical positions and the directions in which they are moving (through the use of GPS [1], RSSI [17], etc.). The MSs' average moving speed is denoted by $\overline{V}$. Thus, the fraction of the total area in a cell that is denoted to be the PR area is given by (see Fig. 2):

$$\alpha = \frac{L_2}{L_1 + L_2} = \frac{E[T_p]\overline{V}}{E[T_n]\overline{V} + E[T_p]\overline{V}}$$
$$= \frac{E[T_p]}{E[T_n] + E[T_p]} = \frac{\eta}{\eta + \gamma}. \tag{3}$$

4.2. An analytical model of the system

We use a $M/M/c$ queuing system [3,15,16] to model the PR scheme in such a one-dimensional cellular system. By using this model, we can compute expressions for the new call blocking probability P_b, the handoff call dropping probability P_d and the call incompletion probability P_{nc}. We take the following steps towards computing the metrics of interest.

4.2.1. PR call arrival rate λ_p

Since MSs are uniformly distributed in the region of interest, and the ratio of the PR area to the total cell area is $\alpha = \frac{\eta}{\eta + \gamma}$, the new call arrival rate in a given PR area is $\alpha \lambda_n$, and is $(1 - \alpha)\lambda_n$ in a given non-PR area. We also note that from the memoryless property of the exponential distribution, the residual call holding time τ_c as observed at any given instant has the same probability distribution as the original call holding time T_c.

The mean arrival rate of PR calls in a cell, denoted by λ_p, is then represented by

$$\lambda_p = \alpha(1 - P_b)\lambda_n + (1 - \alpha)Pr(T_c > T_{nn})(1 - P_b)\lambda_n$$
$$+ Pr(T_c > T_p + T_n)(1 - P_d)\lambda_p. \tag{4}$$

The first term on the right hand side of Eq. (4) represents the new calls generated in area $PR(k - 1, k)$ (with reference to cell k in Fig. 1) and area $PR(k + 1, k)$ (with reference to cell k in Fig. 1). The second term takes into account the calls that are generated in either area $NPR(k - 1)$ or area $NPR(k + 1)$, and are continuing when the owners of these calls move either from area $NPR(k - 1)$ into area $PR(k - 1, k)$ or from area $NPR(k + 1)$ into area $PR(k + 1, k)$. The last term reflects those calls that were handoff calls as seen by either cell $k - 1$ or cell $k + 1$, which are continuing when the owners of these calls transgress either from area $NPR(k - 1)$ into area $PR(k - 1, k)$ or from area $NPR(k + 1)$ into area $PR(k + 1, k)$. It is to be noted that the last term takes into account the calls that are either generated in area $PR(k - 2, k - 1)$ or in area $PR(k + 2, k + 1)$, or are handed off from cell $k - 2$ to cell $k - 1$ or from cell $k + 2$ to cell $k + 1$. The exponential properties that we assume enable us to include all these calls in a single term.[2]

---

[2] This is possible since T_{np} and T_p have the same distribution and T_c is exponentially distributed.

$Pr(T_c > T_{nn})$ and $Pr(T_c > T_p + T_n)$ can be expressed as

$$Pr(T_c > T_{nn}) = \int_0^\infty \mu e^{-\mu\tau} \int_0^\tau \eta e^{-\eta u} du\, d\tau = \frac{\eta}{\mu + \eta}, \tag{5}$$

and

$$Pr(T_c > T_p + T_n)$$
$$= \int_0^\infty \mu e^{-\mu\tau} \int_0^\tau \gamma e^{-\gamma u} \int_0^{\tau-u} \eta e^{-\eta v} dv\, du\, d\tau$$
$$= \frac{\gamma\eta}{(\mu + \gamma)(\mu + \eta)}. \tag{6}$$

From Eqs. (4)–(6), we express λ_p in terms of λ_n, P_b and P_d as follows:

$$\lambda_p = \frac{\left[\alpha + (1 - \alpha)\frac{\eta}{\mu+\eta}\right](1 - P_b)\lambda_n}{1 - \frac{\gamma\eta}{(\mu + \gamma)(\mu + \eta)}(1 - P_d)}. \tag{7}$$

4.2.2. Distribution of the channel holding time T_{ch}

The rate at which calls are accepted in a given cell may be expressed as

$$\lambda_0 = (1 - P_b)\lambda_n + (1 - P_d)\lambda_p. \tag{8}$$

The calls that are accepted (consider cell k in Fig. 2) can be classified into three categories:

- New calls that are generated in area $PR(k, k - 1)$ or in area $PR(k, k + 1)$.
- New calls that are generated in area $NPR(k)$.
- PR calls that are generated in areas $PR(k - 1, k)$ or in area $PR(k + 1, k)$.

The first category of calls hold the channel for a time $T_{ch_1} = \min(T_c, T_{np})$. Since both T_c and T_{np} are exponentially distributed, T_{ch_1} is also exponentially distributed. Furthermore the mean value of T_{ch_1} is given by: $E[T_{ch_1}] = 1/(\mu + \gamma)$. The fraction of calls that belong to this category is given by

$$P_1 = \frac{\alpha(1 - P_b)\lambda_n}{\lambda_0}. \tag{9}$$

The second category of calls have a channel holding time that is given by $T_{ch_2} = \min(T_c, T_{nn} + T_p)$. Let $F_{T_{ch_2}}(t)$ be the CDF of T_{ch_2}. From the PDFs and CDFs of T_c, T_{nn} and T_p, we can derive $F_{T_{ch_2}}(t)$ (see Appendix A for details). The fraction of calls that belong to this category is given by

$$P_2 = \frac{(1 - \alpha)(1 - P_b)\lambda_n}{\lambda_0}. \tag{10}$$

The third category of calls have a channel holding time $T_{ch_3} = \min(T_c, T_{p_{k-1}} + T_n + T_{p_k})$. Let $F_{T_{ch_3}}(t)$ be the CDF of T_{ch_3}. The fraction of calls that belong to this category is given by

$$P_3 = 1 - P_1 - P_2 = \frac{(1 - P_d)\lambda_p}{\lambda_0}. \tag{11}$$

Note that in the third category, for those calls that move either from area $NPR(k - 1)$ into area $PR(k - 1, k)$ or from area $NPR(k + 1)$ into area $PR(k + 1, k)$, the channel holding time in cell k is $\min(T_c, T_{p_{k-1}} + T_n + T_{p_k})$ or $\min(T_c, T_{p_{k+1}} + T_n + T_{p_k})$ [3]. For those new calls that are generated in area $PR(k - 1, k)$ or in area $PR(k + 1, k)$, the channel holding time in cell k is $\min(T_c, T_{np_{k-1}} + T_n + T_{p_k})$. Since $T_{p_{k-1}}$ and $T_{np_{k-1}}$ have the same distribution, we can group all the calls into one category.

The CDF of overall channel holding time T_{ch} is then expressed as

$$F_{T_{ch}}(t) = P_1 \cdot F_{T_{ch_1}}(t) + P_2 \cdot F_{T_{ch_2}}(t) + P_3 \cdot F_{T_{ch_3}}(t). \tag{12}$$

The complementary distribution function $F_{T_{ch}}^C(t)$ is

$$F_{T_{ch}}^C(t) = 1 - F_{T_{ch}}(t). \tag{13}$$

In general, T_{ch} is not exponentially distributed. In order to simplify our analysis, the distribution of T_{ch} is approximated by an exponential distribution with a mean value $E[T_{ch}] = 1/\mu_{ch}$. The use of the exponential distribution to approximate T_{ch} has been justified in [2]. As suggested in [2], if we choose the exponential distribution of T_{ch} with mean $(1/\mu_{ch})$ that satisfies the following condition:

$$\int_0^\infty \left[F_{T_{ch}}^C(t) - e^{-\mu_{ch}t}\right] dt = 0, \tag{14}$$

then, the chosen distribution will approximate the actual distribution very well (as elaborated in [2]). To justify our approximation, we perform simulations that show that our simplification does not significantly alter the behavioral trends of the system.

4.2.3. Problem formulation

Let us assume that the number of channels in each cell is c, and that each of these channels can accommodate a single call. The system is analyzed using a $M/M/c$ queue since the arrival of calls in a

---

[3] Since $T_{p_{k-1}}$ and $T_{p_{k+1}}$ have the same distribution, $\min(T_c, T_{p_{k-1}} + T_n + T_{p_k})$ and $\min(T_c, T_{p_{k+1}} + T_n + T_{p_k})$ also have the same distribution. We use the first expression in the rest of the paper.
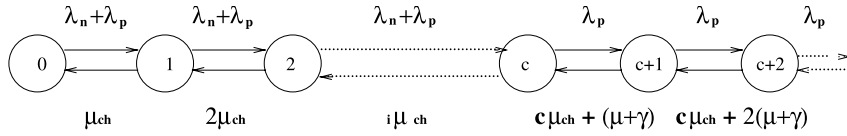
Fig. 3. State transition diagram.

given cell is in accordance to a Poisson process, and the service time T_{ch} is approximated by an exponential distribution. The cell state is represented by $S(k)$, where $k \geqslant 0$ represents the number of calls in the cell. The state transition diagram is shown in Fig. 3. When $0 \leqslant k < c$, the call arrival rate while in state $S(k)$ is $\lambda_n + \lambda_p$; there are k channels that are allocated, and hence, the channel release rate is $k \cdot \mu_{ch}$. When $k \geqslant c$, all the c channels are allocated. At this time new calls that are generated in the cell will be blocked. However, as discussed earlier PR calls are queued.[4] The queueing of PR calls causes the process to transit from $S(k)$ to $S(k+1)$ with rate λ_p. For the c calls that hold channels, the channel release rate is $c \cdot \mu_{ch}$. The $k - c$ calls that are in the queue may be completed or the owners of these calls may move from the PR area into the new cell, prior to channel allocation, which causes the queued call to be dropped. The first effect causes the calls in our $M/M/c$ queue to depart at a rate μ, while the second causes the calls in the queue to depart at a rate γ. Thus, the rate at which the system transits from state $S(k)$ to state $S(k-1)$ is given by $c\mu_{ch} + (k-c)(\mu + \gamma)$.

Let p_i be the probability that the system is in state $S(i)$ at stochastic equilibrium. Then p_i is given by [3,15,16]

$$p_i = \begin{cases} \dfrac{(\lambda_n + \lambda_p)^i}{i! \mu_{ch}^i} p_0 & 0 \leqslant i \leqslant c, \\[3mm] \dfrac{(\lambda_n + \lambda_p)^c \lambda_p^{i-c}}{c! \mu_{ch}^c \prod_{1 \leqslant j \leqslant i-c}[c\mu_{ch} + j(\mu + \gamma)]} p_0 & i > c. \end{cases}$$
(15)

Given $\sum_{i=0}^{\infty} p_i = 1$, p_0 and p_i $(i > 0)$ can be calculated.

A new call is blocked when it arrives at a cell and is unable to find an idle channel. The blocking probability for new calls is given by

<hr>

[4] Note that the queued calls would need to be allocated channels before the owners of these calls actually move into the cell under consideration.

$$P_b = \sum_{i=c}^{\infty} p_i = 1 - \sum_{i=0}^{c-1} p_i.$$
(16)

Let us consider a PR call, PR_t, that arrives in a given cell at a time t when the cell is in state $S(c+j)$, i.e., the cell is operating at capacity and there are j handoff calls in the queue awaiting service. Let the owner MS of this call actually leave this cell at a time $t + \tau$. In this example, τ is PR_t's PR area dwell time, and it has the same distribution as T_p. Let the first time instance when one of the prior calls in service (that occupy the $M/M/c$ queue) in the cell of interest departs (either because it is completed, or it is dropped or because its owner leaves the cell) be denoted by $t + t_{c+j}$. Similarly, let the time instance when the ith $(i \leqslant j+1)$ call (in service) departs from the $M/M/c$ queue be denoted by $t + \sum_{k=0}^{i-1} t_{c+j-k}$. The probability density function of t_{c+k} is given by

$$f_{c+k}(t_{c+k}) = [c\mu_{ch} + k(\mu + \gamma)]e^{-([c\mu_{ch} + k(\mu+\gamma)]t_{c+k})}.$$
(17)

In order for PR_t to be accommodated before time $t + \tau$, it is essential that at least $(j+1)$ of the prior calls that occupy the queue depart before this time. If this does not happen, PR_t is dropped. Thus, the dropping probability of a call PR_t that arrived to a cell that was in state $S(c+j)$ is given by (using Eq. (17))

$$Pr[\tau < t_c + \cdots + t_{c+j} \quad \text{and} \quad \tau > T_c | S(c+j)]$$
$$= \int_{t_c=0}^{\infty} \cdots \int_{t_{c+j}=0}^{\infty} \int_{\tau=0}^{t_c+\cdots+t_{c+j}} \gamma e^{-\gamma \tau} \int_0^{\tau} \mu e^{-\mu T_c}$$
$$\cdot \left[\prod_{k=0}^{j} f_{c+k}(t_{c+k}) \right] dT_c \, d\tau \, dt_c \cdots dt_{c+j}$$
$$= \frac{(j+1)\gamma}{c\mu_{ch} + (j+1)(\mu + \gamma)}.$$
(18)

The dropping probability P_d is then given by

$$P_d = \sum_{j=0}^{\infty} Pr[\tau < t_c + \cdots + t_{c+j} \quad \text{and}$$
$$\tau > T_c | S(c+j)]p_j$$
$$= \sum_{j=0}^{\infty} \frac{(j+1)\gamma p_j}{c\mu_{ch} + (j+1)(\mu + \gamma)},$$
(19)

where p_j are specified as per Eq. (15).

In a time duration $\Delta\tau$, there are $\lambda_n\Delta\tau$ new calls that are generated in a cell. These new calls generate $\lambda_p\Delta\tau$ PR calls in neighboring cells. Among these $(\lambda_n + \lambda_p)\Delta\tau$ new and PR calls, the number of blocked or dropped calls is given by $\lambda_n\Delta\tau P_b + \lambda_p\Delta\tau P_d$. Consequently, the *call incompletion probability* P_{nc} can be expressed as

$$P_{nc} = \frac{\Delta\tau(P_b\lambda_n + P_d\lambda_p)}{\Delta\tau\lambda_n} = P_b + \frac{\lambda_p}{\lambda_n}P_d. \qquad (20)$$

This denotes the fraction of the $\lambda_n\Delta\tau$ arriving calls that are not completed.

4.3. Numerical results

Eqs. (4), (8)–(12), (14)–(16) and (19) form a set of simultaneous non-linear equations. These equations can be solved numerically (via a recursive methodology). The input parameters are c, λ_n, μ, η, γ, and initial choices for P_b, P_d and λ_p (P_b, P_d and λ_p are set to be 0 initially). For all the cases that are considered, the iteration procedures converge since the system under consideration is stable.

We now provide numerical examples to illustrate the effect of PR area size on the overall system performance. We consider two cases: scenarios of low mobility in which $E[T_c] = E[T_n + T_p]$ (i.e., $\mu = \frac{\eta\gamma}{\eta+\gamma}$) and scenarios of high mobility in which $E[T_c] = 3 \cdot E[T_n + T_p]$ (i.e., $3\mu = \frac{\eta\gamma}{\eta+\gamma}$). By low mobility we mean that the average velocity $\overline{V}$ is small and thus a call may last for a duration that is comparable to the time that a MS dwells in a cell. A high mobility pattern indicates that the average velocity is much higher and that the MS might traverse multiple cells, on average, before the call terminates. The number of channels that each cell supports is $c = 20$ and the average call holding time is $E[T_c] = 1/\mu = 360$ s. The normalized traffic load (normalized Erlang load) is defined as $\lambda_n/(c \cdot \mu)$. The performance results are shown for various values of α.

From Figs. 4(a) and 5(a) we see that with an increase in the PR area size from $\alpha = 0$ to $\alpha = 0.1$ ($\alpha = 0.05$ in Fig. 5(a)), P_d decreases. This is because the queued pre-reservation requests are sustained by means of longer queuing times (their dwell time in PR area is prolonged). However, beyond this point, an increase in the size of the PR area leads to a higher P_d. The reason is that with a large PR area size, a high number of false PR requests are generated. It seems like $\alpha = 0.1$ in Fig. 4(a) and $\alpha = 0.05$ in Fig. 5(a) are good values to choose for

determining the PR area size for the respective chosen traffic conditions (see Fig. 7).[5] We also see that in Fig. 5(a), the PR scheme does not help much in decreasing P_d when the speeds of motion are high.

Figs. 4(b) and 5(b) show that P_b increases dramatically with an increase in the PR area size. Since P_b increases dramatically with an increase in the size of the PR area, as per the definition of call incompletion probability, P_{nc} has the same tendency as P_b, i.e., P_{nc} increases dramatically as we increase the size of the PR area (see Figs. 4(c) and 5(c)). Notice that the behavior of neither P_b nor P_{nc} changes by much as we change from a scenario that is based on a low mobility pattern to one that is based on a high mobility pattern. This shows that these metrics are relatively insensitive to vehicular speed.

Fig. 6 shows that the analytical values computed as per Eqs. (16) and (19) for P_b and P_d fit the simulation results very well when $\alpha = 0.1$. We compared analytical results with simulation results for all the cases that we study in this paper, and found that the results for P_b are almost in total agreement in all of the cases, and the results of P_d are also in agreement when $0 \leqslant \alpha \leqslant 0.2$ with scenarios based on low mobility patterns and $0 \leqslant \alpha \leqslant 0.5$ in scenarios based on high mobility patterns.[6]

In Fig. 7, we compare the analytical results with simulation results for various values of α under the two mobility patterns. In the simulations there are 10 cells in the network. The size (length) of each cell is 1800 m. In order to avoid border effects, when a MS moves out of the coverage area of the system, it re-enters the system from the other side. MSs are generated according to a Poisson process (with an average arrival rate of $N_{cell} * \lambda_n/\mu$), where N_{cell} is the number of cells in the system. After a MS is generated, it randomly chooses a location within the service area of the system and a moving direction (left or right). A random moving speed within $[0, V_{max}]$ is also chosen for the MS. With the low mobility pattern, V_{max} is set to 10 m/s and $V_{max} = 30$ m/s with the high mobility pattern. The MS also chooses a life time (or call holding time) as per an exponential distribution (with a mean value of 360 s). It then moves

---

[5] It is difficult to derive the optimal value of α analytically since a set of equations has to be recursively solved. We instead provide two examples with different mobility patterns to illustrate their effect on α.

[6] These results demonstrate the appropriateness of the various assumptions that were made in our analytical formulations to ensure the tractability and simplicity of the analysis.
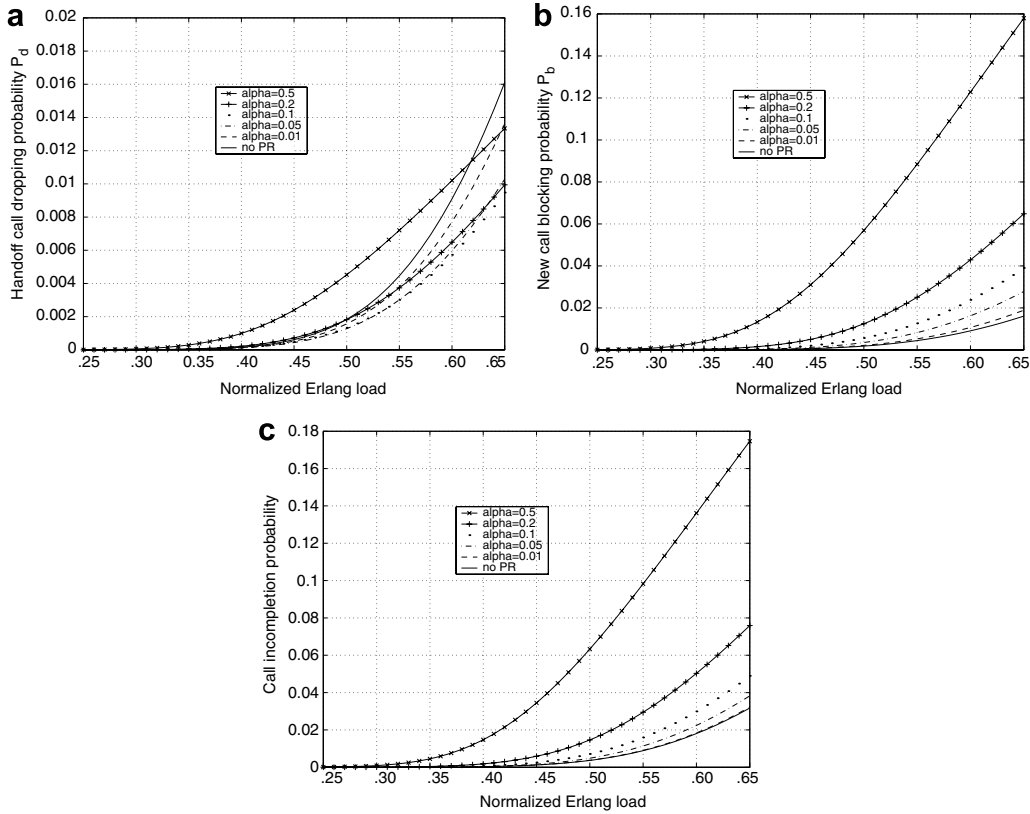
Fig. 4. Analytical results of P_d, P_b and P_{nc} (low mobility pattern). (a) Handoff call dropping probability P_d, (b) new call blocking probability P_b, (c) call incompletion probability P_{nc}.

within the system as per the specified parameters. After its call is terminated (or is dropped), the MS is removed from the system. Note that the length of the simulation is 10 800 s and the number of simulation runs is 50. From Fig. 7, we see that the simplified exponential distribution assumptions of a MS's dwell time in different areas have some effects on the results from the analysis. Specifically, when the size of pre-reservation area is large, the difference between the simulations results and the analytical results is non-negligible. However, our interests are not in this regime of operation. We wish to point out that for low to moderate value of α, the analytical results match well with the simulation results. The behavioral traits are about the same and at the point where performance is best (lowest P_d), the analytical results and the simulation results are in close conformance.

In a nutshell, our results demonstrate that if the reserved channels are strictly mapped to the reserving MSs, increasing the PR area size does not always decrease the handoff call dropping probability. Too small a PR area size will not provide PR requests with an enough queuing time. On the other

hand, too large a PR area size will cause a large number of false reservations and longer channel holding times, and thereby, will increase the handoff call dropping probability. There exists an optimal PR area size (or range of sizes), at which the handoff call dropping probability is minimized. The optimal size of the PR area is closely related to the MSs' mobility pattern (moving speed).

5. Simulations with two-dimensional cellular systems

In Section 4 we studied the effect of the PR area size on handoff prioritization performance with one-dimensional traffic using an analytical model. In this section, we evaluate the effect of the PR area size on the performance of handoff prioritization in two-dimension cellular networks through simulations.[7] The *non-sharing* approach is again used for reserving channels (as in Section 4).

---

[7] An analytical formulation for such more complex systems becomes much more difficult to construct and hence, we resort to simulations.
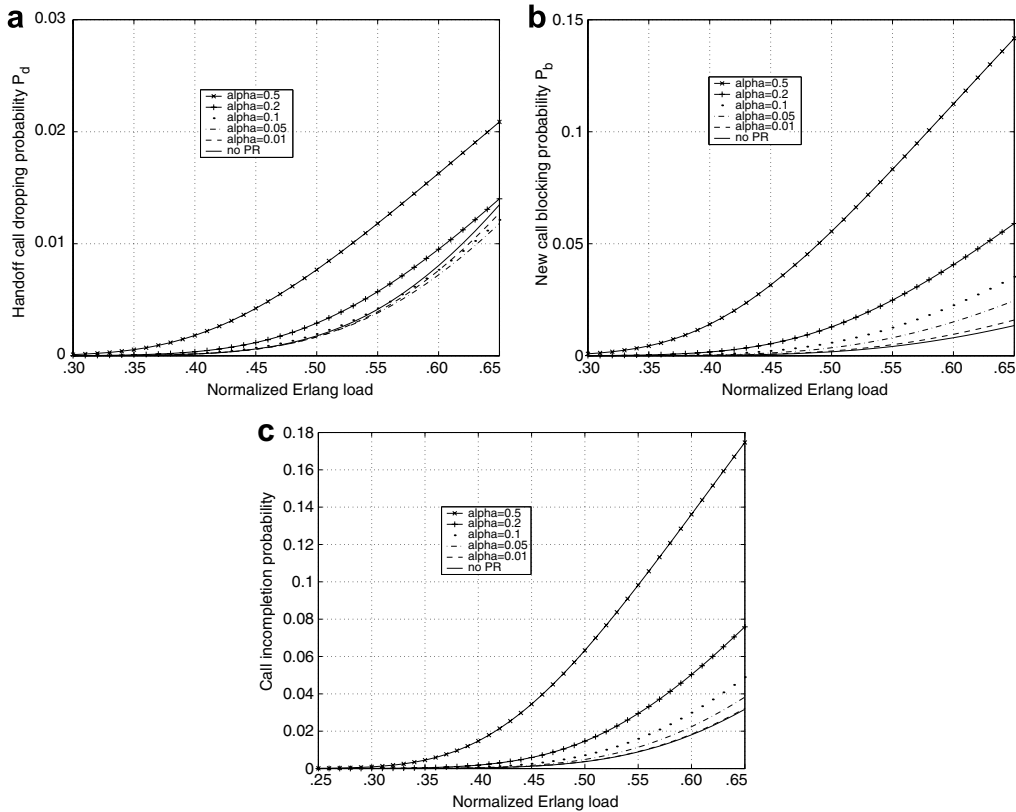
Fig. 5. Analytical results of P_d, P_b and P_{nc} (high mobility pattern). (a) Handoff call dropping probability P_d, (b) new call blocking probability P_b, (c) call incompletion probability P_{nc}.
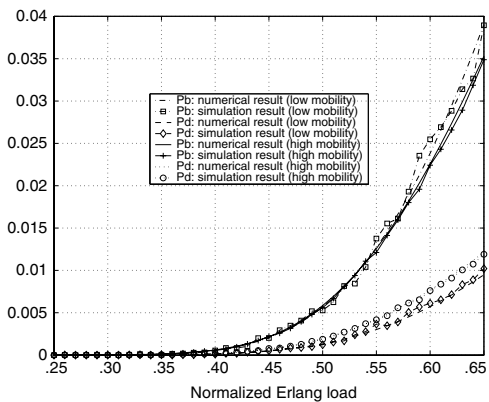

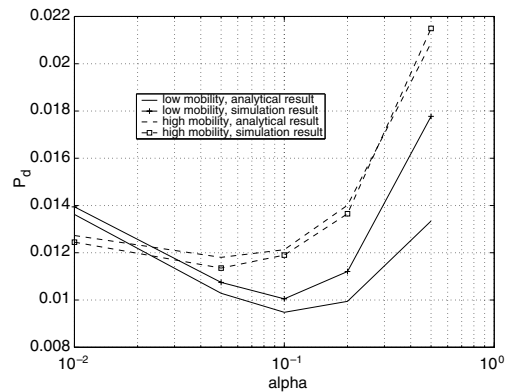Fig. 6. Comparison of analytical results and simulation results ($\alpha = 0.1$).

Fig. 7. Optimal PR area size under different mobility patterns (normalized Erlang load = 0.65).

5.1. Simulation models

The simulation models that we use are discussed below; they include cell shape models, traffic models and mobility models. These models are implemented in CSIM19 [18].

5.1.1. Cell model

The simulations are conducted over a *L* tiered or layered cellular system (see Fig. 8). Square, circular or hexagonal cells are commonly used in the simulation of wireless cellular systems [2]. In our simulations we use hexagons to represent neighborhood
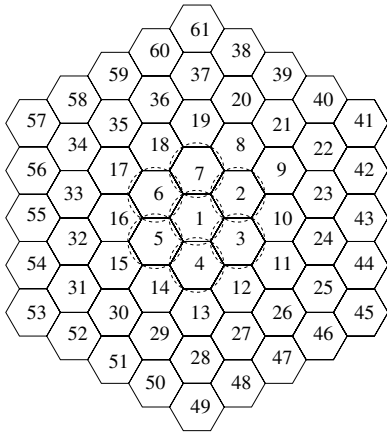
Fig. 8. The topology of a 5-layer wireless cellular system.

relationships among cells and circles to approximate the coverage area of cells. There are overlapping areas between adjacent cells. The radius of each circle (or hexagon) is represented by R_c. There is one central cell in the topology (first layer). The central cell is surrounded by six cells which make up the second layer. There are 12 cells in the third layer, and $6(i-1)$ cells in the ith layer ($1 < i \leqslant L$).

In order to avoid the border effects, we model the system as a toroidal construction such that when a MS moves out of the service area of the system, it re-enters the system from the other side.

5.1.2. Traffic model

Without loss of generality, in our simulations we only consider homogeneous calls and assume that each MS needs only one channel per call. Call generation in the system is as per a Poisson process with an average arrival rate λ. The call holding time T_c follows an exponential distribution with an average service rate μ_c. The number of channels in each cell is a constant c. The normalized offered traffic load on the system is

$$\frac{\lambda}{\mu_c \cdot N \cdot c}, \tag{21}$$

where N is the number of cells in the system, and is computed by

$$N = 1 + \sum_{i=2}^{L} 6(i-1) = 3L(L-1) + 1. \tag{22}$$

Note that the load is measured in Erlangs.

5.1.3. Mobility model

Several mobility models, such as the random way-point model and the fluid-flow model are often used to depict MS' moving behavior in simulations and analysis [14,19,13]. In our simulations, we consider both the random way-point model and an additional mobility model that we consider to be more realistic. Since the simulation results that we were observed were similar with both of the mobility models, in this paper we mainly show the results with the second mobility model (the more realistic mobility model) unless otherwise specified. In the second mobility model, when a new call is generated, the MS initially chooses a speed which is uniformly distributed over $[V_{min}, V_{max}]$ and a moving direction which is uniformly distributed over $[0, 360°]$. In each variable-length period T_u (which is exponentially distributed with mean $E[T_c]/3$),[8] the MS moves along a straight line. After that period, the MS may stop (with a probability P_{stop}) for a time T_u or continue to move (with a probability $P_{cont.} = 1 - P_{stop}$). If the MS continues to move, it may change its direction of motion and speed. The MS makes $\pm 90°$ turns with probability $P_{90°}$, makes $\pm 45°$ turns with probability $P_{45°}$, and moves along the original direction of motion with probability $P_{0°} = 1 - (P_{90°} + P_{45°})$. We believe that this mobility model captures better the realistic scenarios where drastic changes in the direction of motion (>90°) are rare. In fact, this property is captured in some recently proposed mobility models [20]. The Freeway and the Manhattan mobility models are the examples of such models that exhibit this property. In order to be exhaustive, we also provide later, some results that are obtained by allowing MS to change the direction of motion freely.

In order to evaluate the effects of speed patterns on system performance, three different speed patterns are defined.

- *V1 (Low speed):* $V_{min} = 1$ m/s and $V_{max} = 5$ m/s.
- *V2 (Medium speed):* $V_{min} = 6$ m/s and $V_{max} = 10$ m/s.
- *V3 (High speed):* $V_{min} = 11$ m/s and $V_{max} = 20$ m/s.

The use of non-zero minimum speed avoids the undesirable effects of the random waypoint model (as discussed in [21]).

In our simulations we vary the ratio of $R_p - R_c$ to R_c (shown in Fig. 1) to study the effect of PR area

---

[8] We also investigate the effect of varying T_u on the performance later.

Table 1
Parameter values in the simulation

Parameter	Value	Description
L	5	Number of cell layers
R_c	500 m	Cell radius
c	20	Number of channels in each cell
T_c	180 s	Call holding time
P_{stop}	0.1	Probability with which a MS stops
$P_{cont.}$	0.9	Probability with which a MS continues motion
$P_{0°}$	0.7	Probability of keeping original moving direction
$P_{45°}$	0.1	Probability of making a 45° turn
$P_{90°}$	0.2	Probability of making a 90° turn
T_{sim}	10 800 s	Length of simulation
N_{tries}	50	Number of simulation runs

size on handoff prioritization performance. We denote this ratio by α as discussed earlier. The values of the parameters used in our simulations are listed in Table 1.

5.2. Simulation results

Fig. 9 shows the three probability metrics with the low speed pattern V1.[9] Note that if we increase the size of the PR area, initially the handoff dropping probability P_d drops. However, beyond a certain point (e.g., $\alpha \geqslant 0.05$), P_d begins to increase. The following factors affect system performance:

1. A larger PR area allows for PR requests to be queued for longer times if the channels of a cell are temporarily unavailable.
2. A larger PR area causes a channel being reserved by a call, to be held for a longer time.
3. A larger PR area causes a higher number of PR requests and therefore a larger number of false reservations.

The first factor helps decrease P_d while the other two factors increase P_d. The behavioral pattern of variations of the probabilities in Fig. 9 is due to the combined effects of these three factors. As expected, the new call dropping probability P_b increases with an increase in the PR area size. Note that the size of the optimal PR area is very small as compared to the coverage area of the cell.

Figs. 10 and 11 show the effect of PR area size with medium speed pattern V2 and high speed pattern V3, respectively.[10] The observations are similar to those in Fig. 9. Even though the optimal region of operations varies with the pattern of motion and the traffic load, the variations in α are small (α varies from 0.04 to 0.1). Note that the existence of the optimal α allows the cellular network providers to configure the network to provide the best handoff performance.

5.3. Effect of mobility

In order to gain a better understanding on the effect on the mobility of MSs on the handoff performance, we also conduct simulations to quantify its effect. In these simulations, the mobility model that we use is the random waypoint model with a constant non-zero speed as discussed earlier. The normalized Erlang load of the cellular system is 0.7. Fig. 12 shows the results of these simulations. We see that under different speeds of MSs, the optimal regime of operations (i.e., α) is different. As expected, the higher the speed of a MS, the larger the size of the PR area that is needed, in order to ensure that reservation is effectively performed before the MS moves into the new cell. For example, when the speed of MSs is 1 m/s, the optimal α is 0.02; when the speed of MSs is increased to 10 m/s, the optimal α is increased to 0.1. Also, as we discussed earlier, the handoff call probability (Fig. 12(a)) is very sensitive to the size of the PR area (α).

As with our observations with one-dimensional cellular systems, the simulation results with two-dimensional cellular systems also show that there exists an optimal PR area size at which the handoff call dropping probability is minimized. The size of the optimal PR area is closely related to the MSs' mobility patterns (moving speed) and the system load. The observations with the two-dimensional cellular systems further substantiate our observations in Section 4.

6. An adaptive channel reservation scheme

The predictive channel reservation (PCR) scheme is proposed in [1] and it is based on mobile

---

[9] Error bars are shown only for some of the simulation results. Since we collect our results from a large number of simulation runs, the standard derivation is observed to be small and the confidence of our results is high. The errors observed for other simulation experiments were of the same order.

[10] The figures with P_{nc} are not provided since the results obtained are very similar to the results reported for P_b.
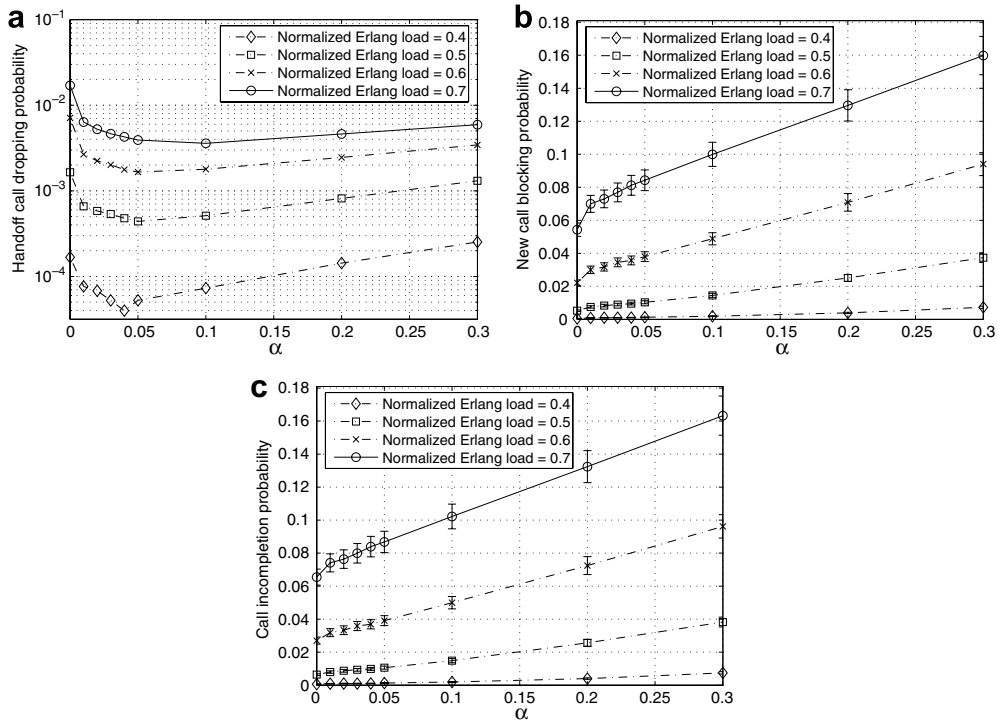
Fig. 9. Effects of variations in the PR area size (in terms of α) on the handoff prioritization performance under speed pattern V1 (Low speed). (a) Handoff call dropping probability P_d, (b) new call blocking probability P_b, (c) call incompletion probability P_{nc}.
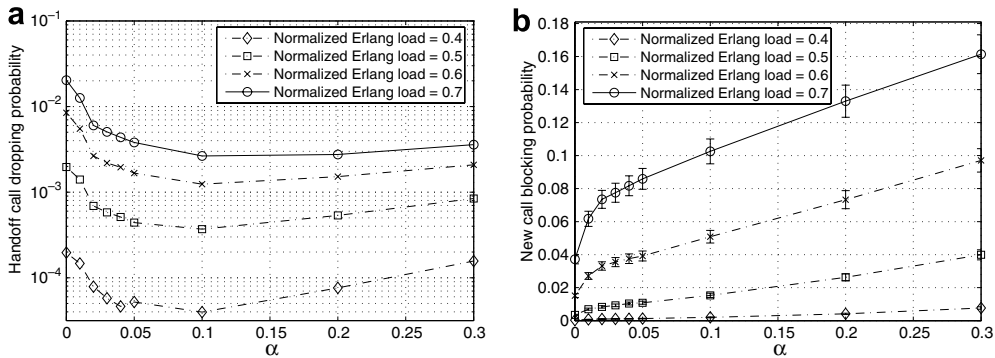

Fig. 10. Effects of variations in the PR area size (in terms of α) on the handoff prioritization performance under speed pattern V2 (medium speed). (a) Handoff call dropping probability P_d, (b) new call blocking probability P_b.

positioning. The *threshold distance* concept (see Fig. 13 and its definition below) is used to define the size of channel PR area. The *threshold distance* (D_{th}) is defined as the radius of a circle beyond which pre-reservations are allowed. This circle is co-centered with a cell, and is smaller than the cell's coverage area (the circle which is drawn with a dashed line in Fig. 13(a)). The area between these two circles is the channel PR area. When a MS enters the PR area of a cell from the inner part of that cell (or if a new

call is generated inside the PR area), and at the same time, is heading to a new cell, a PR request is sent to the base station of that new cell. There are some problems in the PCR scheme. We discuss these in the following paragraphs.

Suppose there is a MS located in the overlapping area of two adjacent cells (see Fig. 13(a)); let the moving speed of this MS be very small (close to 0). If the PCR scheme is used, two channels (each cell has one channel occupied) will be occupied by
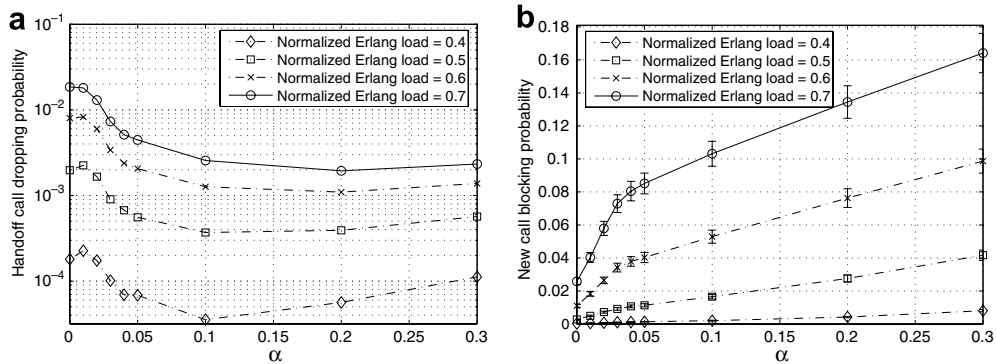
Fig. 11. Effects of variations in the PR area size (in terms of α) on the handoff prioritization performance under speed pattern V3 (high speed). (a) Handoff call dropping probability P_d, (b) new call blocking probability P_b.
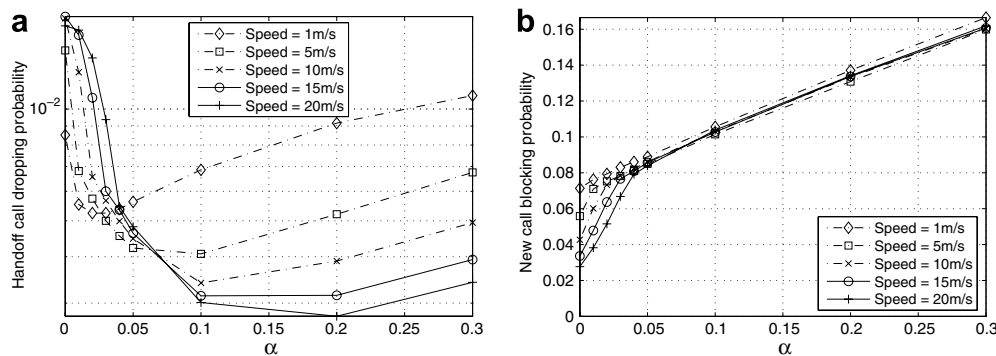

Fig. 12. Effects of the mobility of MSs on the handoff prioritization performance with the random waypoint model. (a) Handoff call dropping probability P_d, (b) new call blocking probability P_b.

this call; one channel is used for communication in the current cell and the other is reserved for this call in the adjacent cell. Since the MS of this call is almost stationary, the reserved channel may not be used for the life time of this call. Naturally, this effect further increases the under-utilization of wireless channels.

A second associated problem is the sensitivity of the performance to the pre-reservation area as seen in our previous studies. A fixed "constant" choice for this area may not be appropriate since mobile users are likely to move with different speeds and orientations. In order to solve the above-mentioned problems that are associated with the PCR scheme, in this section we propose a new handoff prioritization scheme, which we call the adaptive channel reservation (ACR) scheme. The ACR scheme uses the *threshold time* concept to minimize the effect of false reservations and thus, improves the channel utilization of the cellular system. Like the PCR scheme, the ACR scheme is also based on GPS mea-

surements [22]. We do not discuss GPS further in this paper, and just make an assumption that each MS is equipped with GPS and can obtain its precise position information in real-time.

6.1. Threshold time

In the ACR scheme, channel reservation decisions are made based not only on each MS's current position and orientation, but also on the *radial speed* of the MS with respect to its next target cell. The radial speed of a MS with respect to a particular cell is the magnitude of the velocity component of V in the direction from the MS to the cell center (i.e., V_1 in Fig. 13(b)).

Each MS measures its coordinates periodically at regular time intervals (every ΔT seconds[11]) using

---

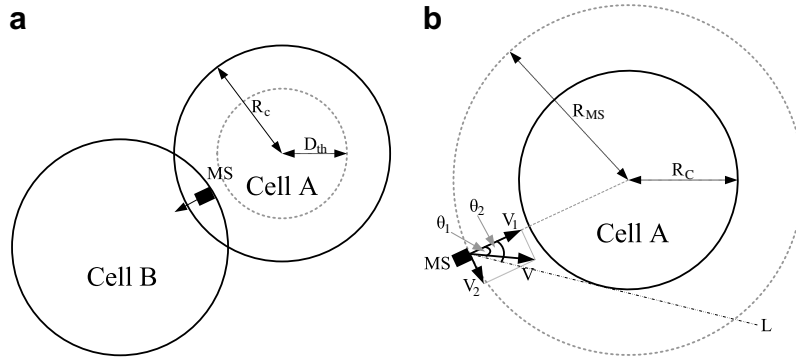[11] In this paper, we use $\Delta T = 1$ s since the typical maximum GPS update frequency is 1 s.

Fig. 13. Illustration of the PCR and ACR schemes. (a) Threshold distance in the PCR scheme, (b) threshold time in the ACR scheme.

GPS. The coordinate information is piggybacked onto uplink data packets (or sent to the associated BS by means of special uplink packets). The BS keeps track of each MS's previous positions, predicts its trajectory [12] and calculates the radial speed with respect to the next cell that the MS is predicted to enter. Based on these calculations, the time within which the MS will reach this candidate cell is predicted.

Threshold time (T_{th}) is a constant time value. As dictated by each MS's current speed of motion, orientation and location information, BSs can estimate the time within which the MS will reach the boundary of its next target cell. In Fig. 13(b), a MS is moving with a velocity V towards cell A. The velocity V can be decomposed into two orthogonal component vectors, V_1 and V_2, where V_1 is the radial velocity component of this MS towards the center of cell A. From V_1 and R_{MS} (the distance between the MS and the center of cell A), the time T_p by which the MS will reach the boundary of cell A is estimated to be

$$T_p = \frac{R_{MS} - R_c}{V_1}, \tag{23}$$

where R_c is the radius of cell A.

Note that with this estimation, the MS is still not guaranteed to enter the target cell. This is simply because by just considering one of the orthogonal velocity components (in this case V_1), one cannot deduce whether the MS is going to enter the target cell or not. Therefore, one should also consider the direction of motion of the MS in making decision. An illustrative example is shown in Fig. 13(b). In the figure, a MS is moving with velocity V. As discussed previously, the velocity vector V is decomposed into V_1 and V_2. We define two

angles: (1) θ_1 is the angle between vector V_1 and vector V, (2) θ_2 is the angle between vector V_1 and line L (the line from the MS tangential to cell A). If $\theta_1 > \theta_2$, one can conclude that with the particular direction the MS will not going to move into cell A and thus, in this case no reservation is made; otherwise, one can conclude that the MS may reach cell A in the time T_p as per Eq. (23).

If $T_p > T_{th}$, it means that the MS may take a time longer than T_{th} to reach cell A, and it does not need a channel reservation in that cell at the current time. If $T_p \leqslant T_{th}$, it means that the MS under consideration will move into cell A soon, and a PR request will be sent by the current BS to cell A's BS. Consider the case when $R_{th} = R_{MS}|_{T_p = T_{th}}$; we call R_{th} the threshold distance for this MS. Note that the threshold distance defined in our paper is different from that in [1] in that different MSs have different threshold distances even though all the MSs have the same T_{th}. This is because they have different radial speeds of motion with respect to any particular given cell.

In summary, a pre-reservation to a given cell is made only if the following two criteria hold:

1. The direction of motion of a MS is towards the cell for which a pre-reservation is to be potentially made.
2. The time within which the MS is estimated to reach the boundary of the cell is smaller than the time threshold T_{th}.

From Sections 4 and 5 we see that if the reserved channels are strictly mapped to the MSs that made the corresponding reservations (i.e., non-sharing approach is used), there exists an optimal pre-reservation area size. The system performance degrades

if the pre-reservation area size is larger than the optimal value. In order to avoid such an effect, in our proposed ACR scheme, the reserved channel sharing approach is used. Note that the idea is not new and has been proposed in [1]. Besides the channel sharing approach, reservation queuing and reservation cancellation, which are used by [1], are also integrated with our threshold time concept to minimize the effect of false reservations and to improve the channel utilization of the cellular system.

As in PCR scheme, the overhead incurred by the ACR scheme is that incurred for the prediction of each MS's future trajectory, the transmission of PR requests and PR cancellation messages that are exchanged between BSs. Since all of these functions are performed by BSs, there is no extra overhead incurred by MSs (for which computation power is limited). The communication overhead (among the BSs) is transmitted over the wire-line network that interconnects these BSs, and does not consume the limited wireless resources.

6.2. Performance of the ACR scheme

The simulation models that are discussed in Section 5 are used in the performance evaluation of the ACR scheme. The values of the parameters used in our simulations are shown in Table 1.

In order to evaluate the performance of the ACR scheme, we also implement the PCR scheme in CSIM19 [18] and compare the performance of the two schemes under the same system conditions.

Fig. 14 shows the values of P_b, P_d and P_{nc} as experienced by the system when the ACR scheme is used with different values of T_{th}. The MSs move in accordance to the speed pattern V1. From Fig. 14(a) it is seen that P_d decreases from 0.1% to 0.02% with an increase in T_{th} (from 3 s to 20 s) when the normalized traffic load is 0.9; the penalty incurred is that, P_b increases from 17% to 22% (see Fig. 14(b)). We also find that P_d is already very small (compared to P_b) even when T_{th} is very small (for example, $T_{th} = 3$ s). The reason for this result is that the overlapping area of a cell with its neighbor-
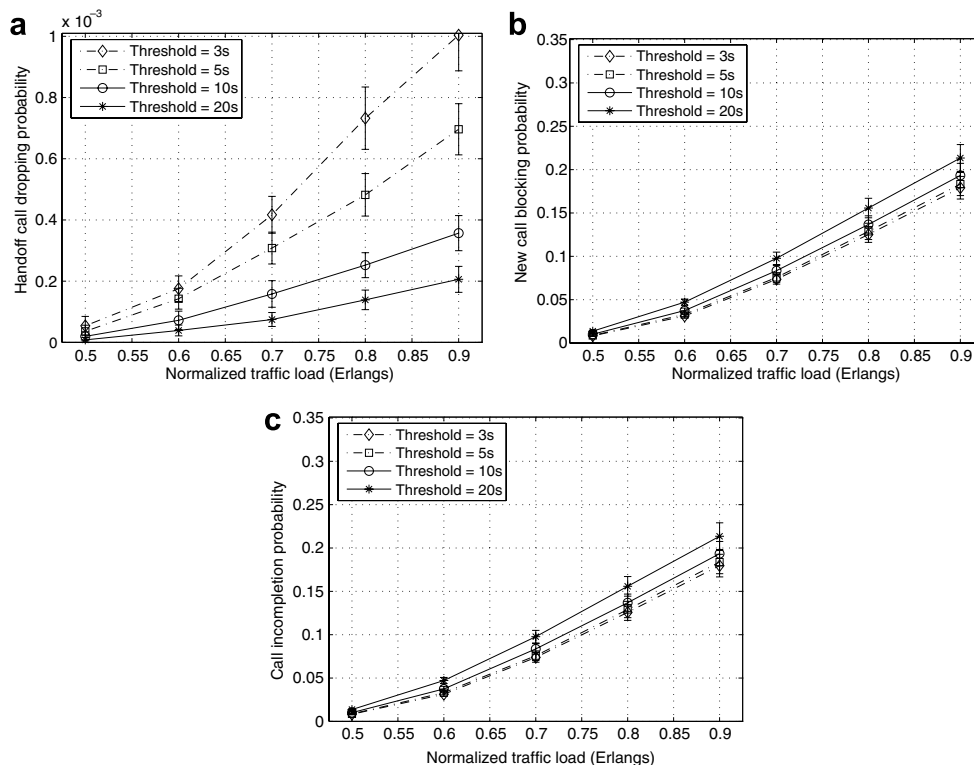

Fig. 14. Performance of the ACR scheme under speed pattern V1 (slow speed). (a) Handoff call dropping probability P_d, (b) new call dropping probability P_b, (c) call incompletion probability P_{nc}.

ing cells contributes to a fairly large portion (about 35%) of the entire cell, and even if a MS cannot access an idle channel before it traverses the boundary of its next cell, it still has a certain period of time (its dwell time in the overlapping area) to wait for an idle channel. So its maximum allowed channel waiting time is larger than T_{th}. Since P_d is much smaller than P_b, most of the unsuccessful calls are new calls (which are blocked). Therefore, the call incompletion probability P_{nc} and the new call blocking P_b are almost the same (see Fig. 14(c)). Note that in the ACR scheme, since the reserved channels can be shared by handoff calls, P_d always decreases with an increase in the PR area (or threshold time), there is no optimal PR area size as was discussed in Sections 5 and 4 for the non-sharing approaches.

Figs. 15 and 16 show the performance of the ACR scheme under two different speed patterns (medium speed pattern V2 and high speed pattern V3). From these two figures, it is seen that P_d under the medium speed pattern is a little higher than that under the high speed pattern. On the other hand, P_b is lower under the medium speed pattern. With a lower speed patterns, the possibility that an ongoing call is handed-off to another cell is smaller than that under higher speed patterns. As a result, under the lower speed pattern, the number of handoffs is smaller, and consequently, the number of reserved channels at any given time is also smaller. Since the ACR scheme is incorporated with reserved channel sharing, the more the number of reserved channels, the lower the probability P_d. This is the reason for P_d being high and P_b being lower under the scenario with the lower speed pattern as compared with the scenario with the higher speed pattern. Another observation is that neither P_d nor P_b is very sensitive to a change in T_{th} under the low speed pattern.
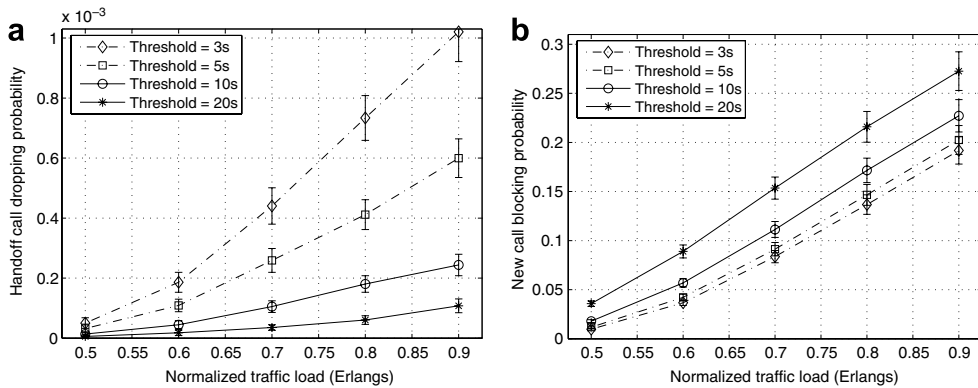

Fig. 15. Performance of the ACR scheme under speed pattern V2 (medium speed). (a) Handoff call dropping probability P_d, (b) new call dropping probability P_b.
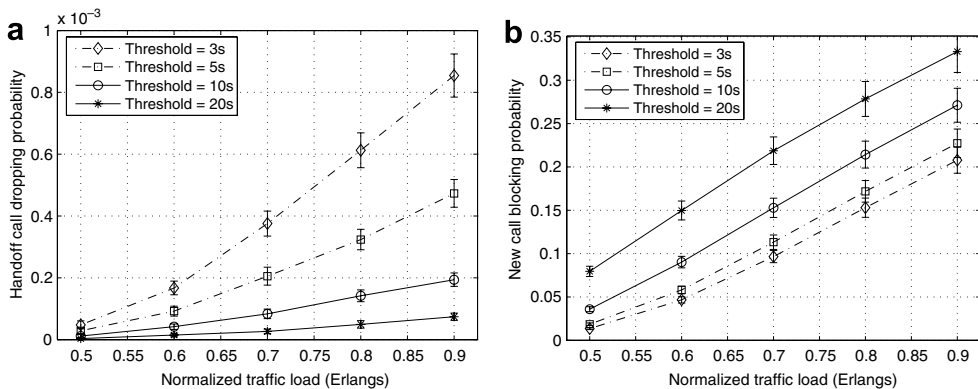

Fig. 16. Performance of the ACR scheme under speed pattern V3 (high speed). (a) Handoff call dropping probability P_d, (b) new call dropping probability P_b.

On the other hand, the sensitivity is much higher under the high speed pattern. It is easy to understand that under high speed pattern, a small increase in T_{th} causes a much larger pre-reservation area than the case under low speed pattern. The increased pre-reservation area causes more pre-reservation requests, which is beneficial to handoff calls (helps to decreases P_d). On the other hand, the increase pre-reservation area blocks more new calls.

Note that there is a tradeoff in selecting the time threshold. A lower time threshold reduces the new call blocking probability and increases the handoff call dropping probability, and vice versa. Since there does not exist an optimal value of the time threshold, the selection of the time threshold will depend on the quality of service (QoS) requirements of the network.

6.3. Effect of mobility

Our next goal is to gain a better understanding on the effect on the mobility of MSs on the handoff performance with the ACR scheme. In our next set of simulations, the mobility model that we use is the random waypoint model with a constant non-zero speed as discussed earlier. The normalized Erlang load of the cellular systems is 0.7. Fig. 17 depicts the results of these simulations. We see that with different chosen speeds, the handoff call dropping probability (P_d) with the ACR scheme does not change by much. Moreover, there does not exist an optimal time threshold value for minimizing P_d. This is in contrast to the observations that we see in Section 5 (Fig. 12). This observation demonstrates that the ACR scheme can actually alleviate the sensitivity of the handoff performance to the threshold time parameter and hence, the threshold distance. Note that this is unlike with PCR where the performance is sensitive to the choice of the threshold distance (depends on an associated parameter α) as discussed earlier.[12]

6.4. Effect of the size of T_u

As discussed, T_u is the variable-length period and is modelled with the exponential distribution. This variable-length period is used to determine the frequency of stops, and the changes in the direction and speed of each MS. It is therefore important to investigate the effects of this parameter on the performance results obtained. We perform simulations with different T_u values and obtain performance results in terms of our metrics of interest. Fig. 18 shows the results P_d and P_b with different mean T_u values. As seen from the results, the smaller the size of T_u (i.e., the more frequent the changes in MSs' motion), the higher the value of P_d. With a high frequency of changes in motion, a MS may reserve a channel but may change its direction of motion later such that the earlier reserved channel is not useful anymore. This is in agreement with the results in Fig. 18(c); here we observe that a smaller T_u leads to a higher false reservation probability. However, as seen in Fig. 18(b), the new call blocking probability remains more or less unchanged for different values of T_u. This is because the average number of reserved channels in a cell (and thus, the average number of free channels in a cell) should still be around the same, given that the distribution of MSs and their average speeds are the same.

The comparison of the ACR scheme with the PCR scheme in terms of performance with the low speed pattern V1 is shown in Fig. 19. By choosing $T_{th} = 3$ s with the ACR scheme and the threshold distance $D_{th} = 0.723R_c$ in the PCR scheme, the two schemes have almost the same P_d for various normalized traffic loads (see Fig. 19(a)).[13] We will say that a scheme outperforms the other if it has a lower P_b.[14] The ACR scheme decreases P_b by up to 40% as compared with the PCR scheme (See Fig. 19(b)). Similarly, by choosing $T_{th} = 20$ s in the ACR scheme and $D_{th} = 0.69R_c$ in the PCR scheme, the two schemes have the same P_d. Correspondingly the value of P_b in the ACR scheme is lower by up to 15% as compared with that seen in

---

[12] We wish to point out that one cannot map α to the threshold time directly without taking into account the speed of the MSs. However, if one makes an assumption with regards to the mobility of MSs (say, the average speed of MSs is V), then α will be approximately equal to $V \times T_{th}$, where T_{th} is the threshold time in the ACR scheme. As we point out in the paper, the ACR scheme alleviates the sensitivity of the speed of the MSs to the handoff performance; the sensitivity is high with the PCR scheme.

[13] Since an exact match between the P_ds is extremely difficult, we try to determine scenarios in which P_ds are almost identical.
[14] We make the P_d of the PCR scheme a little bit higher (as possible) than that of the ACR scheme to actually give an advantage to the PCR scheme when we compare their P_bs. If the P_b with the ACR scheme is lower than that with the PCR scheme, we can confirm that the ACR scheme outperforms the PCR scheme.
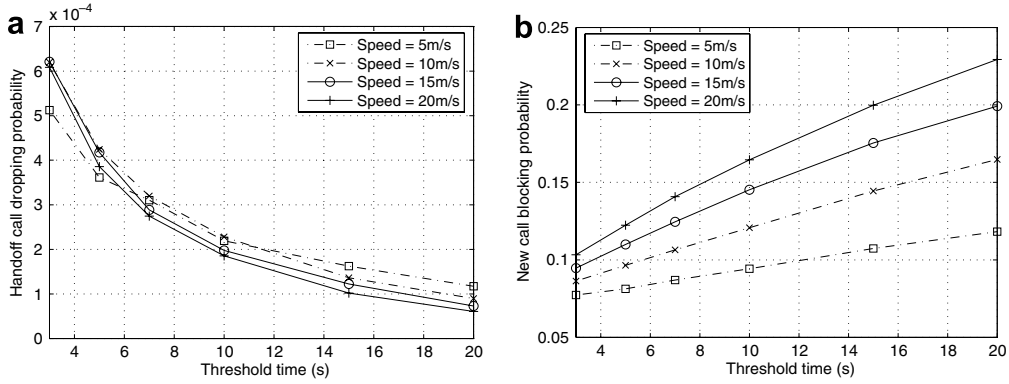
Fig. 17. Effects of the mobility of MSs on the handoff prioritization performance of ACR scheme with the random waypoint model (normalized Erlang load is 0.7). (a) Handoff call dropping probability P_d, (b) new call blocking probability P_b.
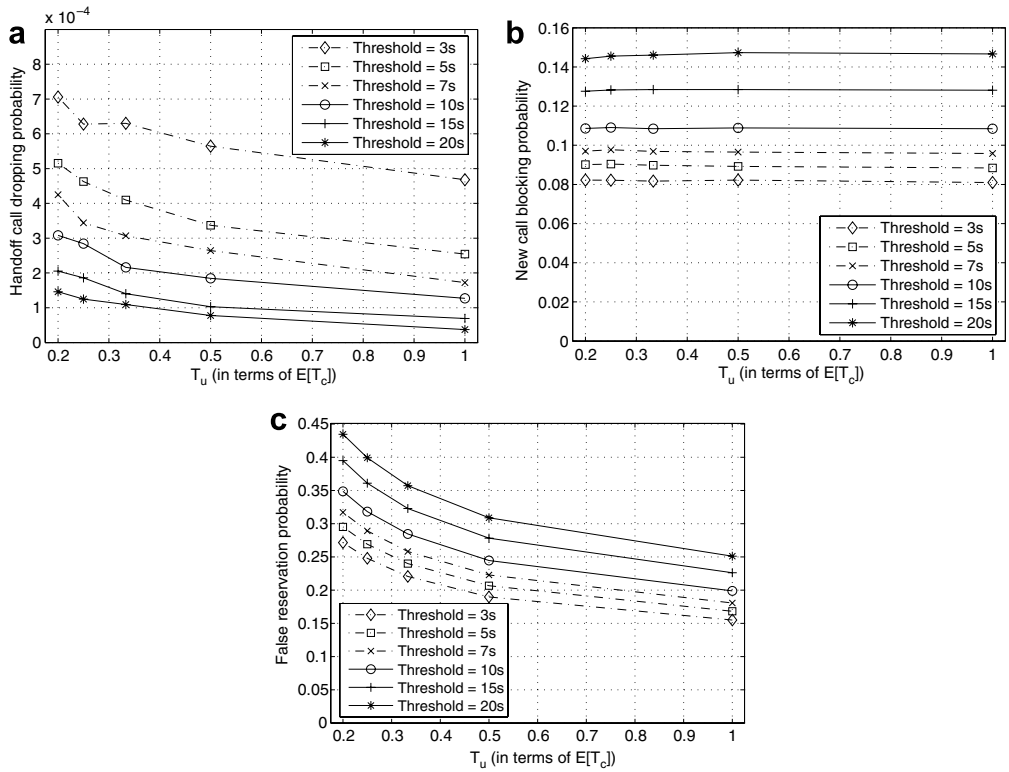

Fig. 18. Effects of the variable-length period T_u (in terms of $E[T_c]$) on the handoff prioritization performance with a normalized Erlang load of 0.7. (a) Handoff call dropping probability P_d, (b) new call blocking probability P_b, (c) false reservation probability.

the PCR scheme. Since the call incompletion probability P_{nc} is dominated by P_b, the ACR scheme can ensure more completed calls than the PCR scheme. Consequently, the ACR scheme achieves a higher channel utilization than the PCR scheme.

Fig. 20 compares the performance of the two schemes under the low speed pattern V2. In

Fig. 20(a), by choosing $T_{th} = 3$ s and $D_{th} = 0.815R_c$, these two schemes have almost the same P_d for various normalized traffic loads. Correspondingly, in Fig. 20(b), P_b with the ACR scheme is lower by up to 8% as compared with that in the PCR scheme. Similarly, by choosing $T_{th} = 20$ s and $D_{th} = 0.76R_c$, the two schemes have almost the same P_d, and P_b
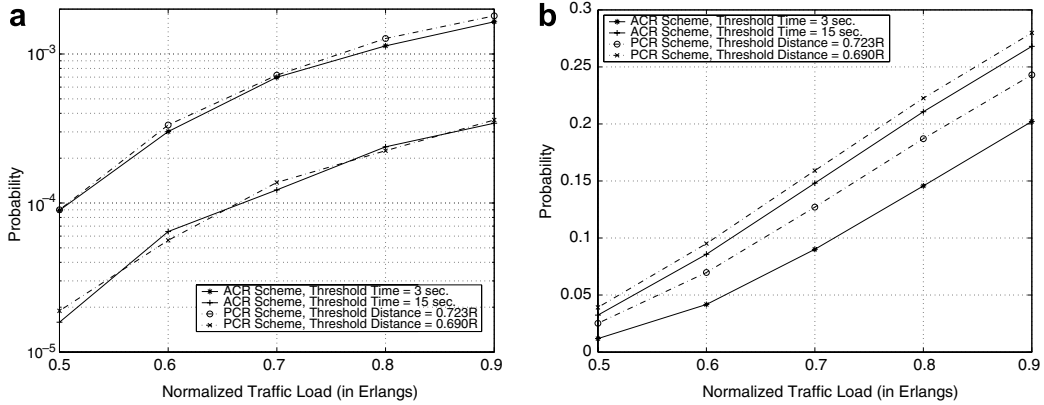
Fig. 19. Performance comparison between the ACR scheme and the PCR scheme under V1. (a) Handoff call dropping probability P_d, (b) new call blocking probability P_b.
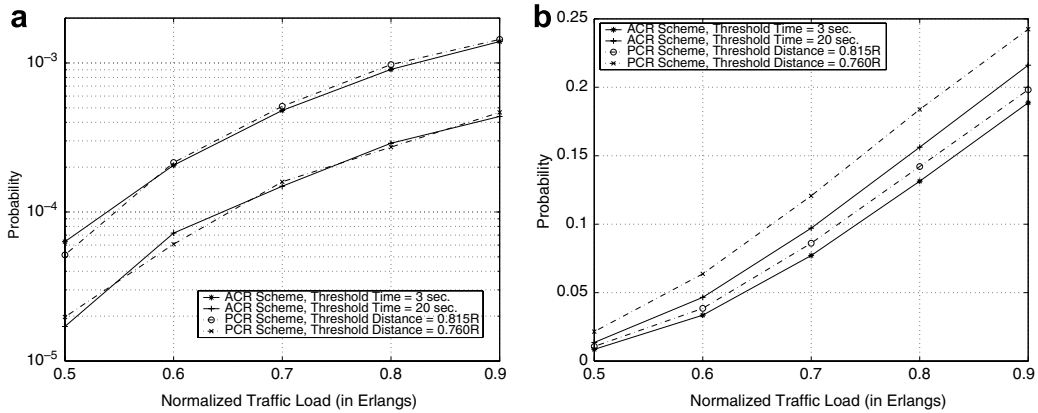

Fig. 20. Performance comparison between the ACR scheme and the PCR scheme under V2. (a) Handoff call dropping probability P_d, (b) new call blocking probability P_b.

with the ACR scheme is lower by up to 27% as compared with that with the PCR scheme. One interesting observation is that P_b with the ACR scheme is much lower with a larger T_{th} under speed pattern V2 (in contrast, P_b is somewhat higher if T_{th} is larger as seen in Fig. 19(a)). Under the low speed pattern, the average number of channel reservation requests is smaller than that under the high speed pattern, while the channel holding time of a call in a given cell is longer. This would imply that the rate at which the occupied channels are released will be smaller if we have a low speed pattern and the reservation request may therefore need a longer time to get an idle channel. For the same value of T_{th} and the same normalized traffic load, P_d under a low speed pattern is higher and P_b is lower than the corresponding values observed under a high speed pattern.

Fig. 21 compares the performance of these two schemes under the high speed pattern. In Fig. 21(a), by choosing $T_{th} = 3$ s and $D_{th} = 0.71R_c$ we ensure that the two schemes have almost the same P_d for various normalized traffic loads. In Fig. 21(b), we see that P_b with the ACR scheme is lower by about 30% as compared with that seen with the PCR scheme. On the other hand, the ACR scheme has almost the same P_d and P_b as the PCR scheme when $T_{th} = 15$ s and $D_{th} = 0.6R_c$. This is due to the fact that under high speed patterns, if T_{th} is large, the channel reservation area will become very large; consequently the fraction of calls that make reservation requests in adjacent cells will be large. The performance of the ACR scheme will therefore deteriorate. However, even in this unrealistic scenario, the ACR scheme still performs as well as the PCR scheme.
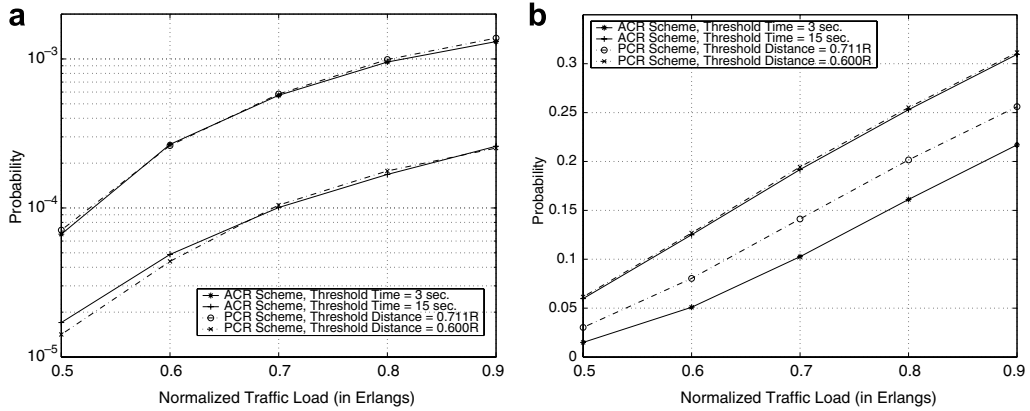
Fig. 21. Performance comparison between the ACR scheme and the PCR scheme under V3. (a) Handoff call dropping probability P_d, (b) new call blocking probability P_b.

Since the ACR scheme is distributed, it can be applied not only in homogeneous systems in which every cell has the same size, shape and number of channels, but also in heterogeneous systems in which each cell might have a different coverage area, a different shape and a varying number of channels. The scheme may be expected to work well under non-uniform traffic loads as well.

7. Conclusions

In this paper, we study different predictive channel reservation schemes for cellular networks and evaluate the effect of pre-reservation size to the handoff prioritization performance. Both the analytical results with one-dimensional cellular networks and the simulation results with two-dimensional cellular systems show that when the reserved channels are not shared by the handoff calls, i.e., when the reserved channel is strictly mapped to the mobile station that made the reservation, there exists an optimal pre-reservation area size, at which the handoff dropping probability is minimized. However, if reservations are pooled, i.e., the set of channels that are reserved are allocated to handoff calls on a first come first served bases, the value of P_d strictly decreases with an increase in the pre-reservation area size. We also propose an adaptive channel pre-reservation scheme that overcomes the deficiencies of the prior pre-reservation schemes. The proposed scheme uses GPS measurements to determine when channel pre-reservations are to be made. The key idea is to send a channel pre-reservation request for a possible hand-off call to a neighboring cell not only based on the position and orientation of the owner mobile station, but also as dictated by the speed of the mobile station towards the target cell. The scheme also integrates reserved channel sharing, reservation queuing and reservation cancellation, which have been proposed and used in the PCR scheme [1], with threshold time concept to prioritize handoff calls and improve the overall channel utilization. Extensive simulations are performed and the simulation results show that our adaptive channel reservation scheme can accommodate more new calls (has lower new call blocking probability) than the previously proposed PCR scheme while maintaining the same value of handoff call dropping probability for any given traffic load.

Appendix A

In this appendix, we derive the probability distribution functions (PDF) and cumulative distribution functions (CDF) of some random variables that are used in this paper.

From Eq. (12) we see that the CDF of the overall channel holding time T_{ch}, denoted by $F_{T_{ch}}(t)$, is expressed in terms of $F_{T_{ch_1}}(t)$, $F_{T_{ch_2}}(t)$ and $F_{T_{ch_3}}(t)$, where $T_{ch_1} = \min(T_c, T_{np})$, $T_{ch_2} = \min(T_c, T_{nn} + T_p)$ and $T_{ch_1} = \min(T_c, T_{p_{k-1}} + T_n + T_{p_k})$. Since both T_c and T_{np} are exponentially distributed with $E[T_c] = 1/\mu$ and $E[T_{np}] = 1/\eta$ respectively, T_{ch_1} is also exponentially distributed with $E[T_{ch_1}] = 1/(\mu + \eta)$. In order to obtain the CDFs of random variables T_{ch_2} and T_{ch_3}, we need to first obtain the CDFs of $T_{nn} + T_p$ and $T_{p_{k-1}} + T_n + T_{p_k}$.

Let $T_d = T_{nn} + T_p$. The PDF and CDF of T_d are

$$f_{T_d}(t) = \int_0^t f_{T_p}(\tau) f_{T_{nn}}(t - \tau) d\tau = \int_0^t \gamma e^{-\gamma\tau} \eta e^{-\eta(t-\tau)} d\tau$$

$$= \begin{cases} \frac{\gamma\eta}{\gamma-\eta}(e^{-\eta t} - e^{-\gamma t}) & \text{if } \eta \neq \gamma, \text{ and} \\ \eta^2 t e^{-\eta t} & \text{if } \eta = \gamma, \end{cases}$$

(A.1)

and

$$F_{T_d}(t) = \begin{cases} 1 - \frac{\gamma e^{-\eta t} - \eta e^{-\gamma t}}{\gamma - \eta} & \text{if } \eta \neq \gamma, \text{ and} \\ 1 - e^{-\eta t} - \eta t e^{-\eta t} & \text{if } \eta = \gamma. \end{cases}$$

(A.2)

Then, the CDF of $T_{ch_2} = \min(T_c, T_{nn} + T_p) = \min(T_c, T_d)$ can be expressed as

$$F_{T_{ch_2}}(t) = F_{T_c}(t) + F_{T_d}(t)[1 - F_{T_c}(t)]$$

$$= \begin{cases} 1 - \frac{\gamma e^{-(\mu+\eta)t} - \eta e^{-(\mu+\gamma)t}}{\gamma - \eta} & \text{if } \eta \neq \gamma, \text{ and} \\ 1 - e^{-(\mu+\eta)t} - \eta t e^{-(\mu+\eta)t} & \text{if } \eta = \gamma. \end{cases}$$

(A.3)

Let $T_x = T_{np} + T_n + T_p = T_{np} + T_d$. The PDF and CDF for T_x are

$$f_{T_x}(t) = \int_0^t f_{T_d}(\tau) f_{T_{np}}(t - \tau) d\tau$$

$$= \begin{cases} \int_0^t \frac{\gamma\eta}{\gamma-\eta}(e^{-\eta\tau} - e^{-\gamma\tau})\gamma e^{-\gamma(t-\tau)} d\tau & \text{if } \eta \neq \gamma, \text{ and} \\ \int_0^t \eta^2 \tau e^{-\eta\tau} \eta e^{-\eta(t-\tau)} d\tau & \text{if } \eta = \gamma. \end{cases}$$

$$= \begin{cases} \frac{\gamma^2\eta}{(\gamma-\eta)^2}[e^{-\eta t} - e^{-\gamma t} - (\gamma-\eta)t e^{-\gamma t}] & \text{if } \eta \neq \gamma, \text{ and} \\ \frac{\eta^3}{2} t^2 e^{-\eta t} & \text{if } \eta = \gamma, \end{cases}$$

(A.4)

and

$$F_{T_x}(t) = \begin{cases} 1 - \frac{\gamma^2 e^{-\eta t}}{(\gamma-\eta)^2} + \frac{\gamma\eta e^{-\gamma t}}{(\gamma-\eta)^2} \\ + \frac{\eta e^{-\gamma t}}{\gamma-\eta} + \frac{\eta\gamma t e^{-\gamma t}}{\gamma-\eta} & \text{if } \eta \neq \gamma, \text{ and} \\ 1 - e^{-\eta t} - \eta t e^{-\eta t} \\ - \frac{\eta^2}{2} t^2 e^{-\eta t} & \text{if } \eta = \gamma. \end{cases}$$

(A.5)

Since $T_{ch_3} = \min(T_c, T_{np} + T_n + T_p) = \min(T_c, T_x)$, by following a methodology similar to the one followed in deriving the CDF $F_{T_{ch_2}}(t)$, we obtain the expression of $F_{T_{ch_3}}(t)$ to be

$$F_{T_{ch_3}}(t) = \begin{cases} 1 - \frac{\gamma^2 e^{-(\mu+\eta)t}}{(\gamma-\eta)^2} + \frac{\gamma\eta e^{-(\mu+\gamma)t}}{(\gamma-\eta)^2} \\ + \frac{\eta e^{-(\mu+\eta)t}}{\gamma-\eta} + \frac{\gamma\eta t e^{-(\mu+\gamma)t}}{\gamma-\eta} & \text{if } \eta \neq \gamma, \text{ and} \\ 1 - e^{-(\mu+\eta)t} - \eta t e^{-(\mu+\eta)t} \\ - \frac{\eta^2}{2} t^2 e^{-(\mu+\eta)t} & \text{if } \eta = \gamma. \end{cases}$$

(A.6)

Using the CDF expressions ($F_{T_{ch_1}}(t)$, $F_{T_{ch_2}}(t)$ and $F_{T_{ch_3}}(t)$) that we thus obtained, we can compute the CDF of the overall channel holding time T_{ch} (see Eq. (12)).

References

[1] M. Chiu, M. Bassiouni, Predictive schemes for handoff prioritization in cellular networks based on mobile positioning, IEEE Journal on Selected Areas in Communications 18 (3) (2000) 510–522.

[2] D. Hong, S. Rappaport, Traffic model and performance analysis for cellular mobile radio telephone systems with prioritized and nonprioritized handoff procedures, IEEE Transaction on Vehicular Technology 35 (3) (1986) 77–92.

[3] Y. Lin, S. Mohan, A. Noerpel, Analyzing queueing priority channel assignment strategies for hand-off and initial access for a pcs network, IEEE Transactions on Vehicular Technology 43 (3) (1994) 704–712.

[4] D. Levine, I. Akyildiz, M. Naghshineh, A resource estimation and call admission algorithm for wireless multimedia networks using the shadow cluster concept, IEEE/ACM Transactions on Networking 5 (1) (1997) 1–8.

[5] N. Tripathi, J. Reed, H. VanLandinoham, Handoff in cellular systems, IEEE Personal Communications 5 (6) (1998) 26–37.

[6] S. Tekinay, B. Jabbari, Handover policies and channel assignment strategies in mobile cellular networks, IEEE Communications Magazine 29 (11) (1991) 42–46.

[7] Y. Kim, D. Lee, Y. Kim, B. Mukherjee, Dynamic channel reservation based on mobility in wireless atm networks, IEEE Communications Magazine (1999) 47–51.

[8] O.T. Yu, V.C.M. Leung, Adaptive resource allocation for prioritized call admission over an atm-based wireless pcn, IEEE Journal on Selected Areas in Communications 15 (7) (1997) 1208–1225.

[9] W. Zhuang, K. Chua, S. Jiang, Measurement-based dynamic bandwidth reservation scheme for handoff in mobile multimedia networks, in: Proceedings of the IEEE International Conference on Universal Personal Communications, 1998.

[10] J. Jobin, S. Tripathi, M. Faloutsos, S. Gokhale, Using statistical data for reliable mobile communications, The Journal of Wireless Communications and Mobile Computing 2 (1) (2002) 101–111 (special issue on Reliable Transport Protocols for Mobile Computing).

[11] V. Bharghavan, J. Mysore, Profile based next-cell prediction in indoor wireless lans, in: Proceedings of the IEEE Singapore International Conference on Networks, 1997.

[12] W. Cui., X. Shen, User movement tendency prediction and call admission control for cellular networks, in: Proceedings of the IEEE International Conference on Communications (ICC), vol. 2, 2000.

[13] H. Xie, S. Tabbane, D. Goodman, Dynamic location area management and performance analysis, in: Proceedings of 43rd IEEE Vehicular Technology Conference, 1993.

[14] B. Liang, Z. Hass, Predictive distance-based mobility management for pcs networks, in: Proceedings of the IEEE INFOCOM, 1999.

[15] Y. Lin, A. Pang, Comparing soft and hard handoffs, IEEE Transaction on Vehicular Technology 49 (3) (2000) 792–798.

[16] Queueing Systems, vol. I, John Wiley and Sons, 1975.

[17] T. Liu, P. Bahl, I. Chlamtac, Mobility modeling, location tracking, and trajectory prediction in wireless atm networks, IEEE Journal on Selected Areas in Communications 16 (6) (1998) 922–936.

[18] http://www.mesquite.com/, Csim19 introduction.

[19] M.M. Zonoozi, P. Dassanayak, User mobility modeling and characterization of mobility patterns, IEEE Journal on Selected Areas in Communications 15 (7) (1997) 1239–1252.

[20] F. Bai, N. Sadagopan, A. Helmy, IMPORTANT: a framework to systematically analyze the impact of mobility on performance of routing protocols for adhoc networks, in: Proceedings of the IEEE INFOCOM, 2003, pp. 825–835.

[21] J. Yoon, M. Liu, B. Noble, Random waypoint considered harmful, in: Proceedings of the IEEE INFOCOM, 2003.

[22] Global Positioning System: Theory and Practice, Springer-Verlag, 1997.

Lap Kong Law received his B.S. degree in Computer Science from The Chinese University of Hong Kong in 2002. He is currently a Ph.D. candidate in the Department of Computer Science and Engineering, University of California, Riverside. His research interests inculde routing protocols for unicast, broadcast and multicast communications in ad hoc networks, TCP performance over wireless networks and capacity analysis of cellular/ad-hoc hybrid networks.

Srikanth V. Krishnamurthy received his Ph.D. degree in electrical and computer engineering from the University of California at San Diego in 1997. From 1998 to 2000, he was a Research Staff Scientist at the Information Sciences Laboratory, HRL Laboratories, LLC, Malibu, CA. Currently, he is an Associate Professor of Computer Science at the University of California, Riverside. His research interests span CDMA and TDMA technologies, medium access control protocols for satellite and wireless networks, routing and multicasting in wireless networks, power control, the use of smart antennas and security in wireless networks. He has been a PI or a project lead on projects from various DARPA programs including the Fault Tolerant Networks program, the Next Generation Internet program and the Small Unit Operations program. He is the recipient of the NSF CAREER Award from ANI in 2003. He has also co-edited the book ''Ad Hoc Networks: Technologies and Protocols'' published by Springer Verlag in 2005. He has served on the program committees of INFOCOM, MOBIHOC and ICC and is the associate editor-in-chief for ACM MC2R.

Zhenqiang Ye received his B.S. and M.S. degrees in electrical engineering from Northwestern Polytechnic University, Xi'An, China in 1992 and 1995, respectively. In 2004 he received his Ph.D. degree in the Department of Electrical Engineering, University of California, Riverside. Currently he is a sensor research engineer in Dust Networks. From 1995 to 1999, he was an electrical engineer with Beijing Institute of Control Engineering, Beijing, China. His research interests are in the design, simulation and performance evaluation of routing, medium access control, and transport protocols for mobile ad hoc networks and wireless sensor networks.

Zhong Xu received his Ph.D. in Electrical Engineering and MS in Computer Science from the University of California, Riverside in 2004 and 2003 respectively. He also received the ME degree (1993) and BE degree (1990) from Southeast University, Nanjing, China. His research interests include TCP congestion control, Internet protocols, network performance evaluation, and distributed systems. Currently, he is a senior engineer at Oracle Inc.
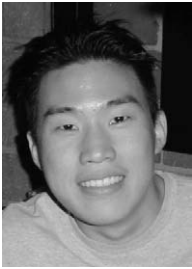
Suvidhean Dhirakaosal received his B.S. in Electrical Engineering from the University of California, Riverside on 2001. In 2004, he received his M.S. in Computer Science from the University of California, Riverside. He is currently working in the embedded systems field as a software engineer at Corelis Inc.

Satish K. Tripathi attended the Banaras Hindu University, the Indian Statistical Institute, the University of Alberta and the University of Toronto. He received Ph.D. in Computer Science from the University of Toronto. He joined the Computer Science faculty at the University of Maryland in 1978. He served as the Department chair During 1988–1995. He has been visiting professor at the University of Paris and University of Erlangen-Nuremberg. He served as the Dean and the Johnson Professor of Engineering at the University of California at Riverside during 1997–2004. Since 2004, he has been the Provost and Executive Vice-President at the University at Buffalo, the State University of New York.

He has been actively involved in research related to performance evaluation, networks, real-time systems and fault tolerance. He has published more than 200 papers in international journals and refereed conferences. In the networking area his current projects are on mobile computing, quality of service routing, network support for multimedia information. He has supervised more than 20 Ph.D. students.

He has served as the member of the Program Committee and Program Chairman for various international conferences. He has guest edited special issues of many journals and serves/served on the editorial boards of Theoretical Computer Science, ACM/Springer Multimedia Systems, IEEE/ACM Transactions on Networking, International Journal of High Speed Networking, IEEE Transactions on Computers, and IEEE Pervasive Computing. He has edited books in the areas of performance evaluation and parallel computing. He coauthored a book on Networked Multimedia Systems. He is a Fellow of both IEEE and AAAS.

Mart L. Molle is a professor in the Department of Computer Science and Engineering at the University of California, Riverside. His research interests include the performance evaluation of protocols for computer networks and of distributed systems. Molle received a B.Sc.(Hons.) in mathematics/computing science from Queen's University at Kingston, Canada, and an M.S. and Ph.D. in computer science from the University of California, Los Angeles.